ChemPubSoc Europe

DOI: 10.1002/chem.201502394

CHEMISTRY
A European Journal
Full Paper

Catenanes |*Hot Paper*|

Reversible Mechanical Interlocking of D-Shaped Molecular Karabiners bearing Coordination-Bond Loaded Gates: Route to Self-Assembled [2]Catenanes

Soumyakanta Prusty,[a] Shobhana Krishnaswamy,[a] Sreenivasulu Bandi,[a] Baby Chandrika,[b] Jingwei Luo,[c, d] J. Scott McIndoe,[d] Garry S. Hanan,[c] and Dillip Kumar Chand*[a]

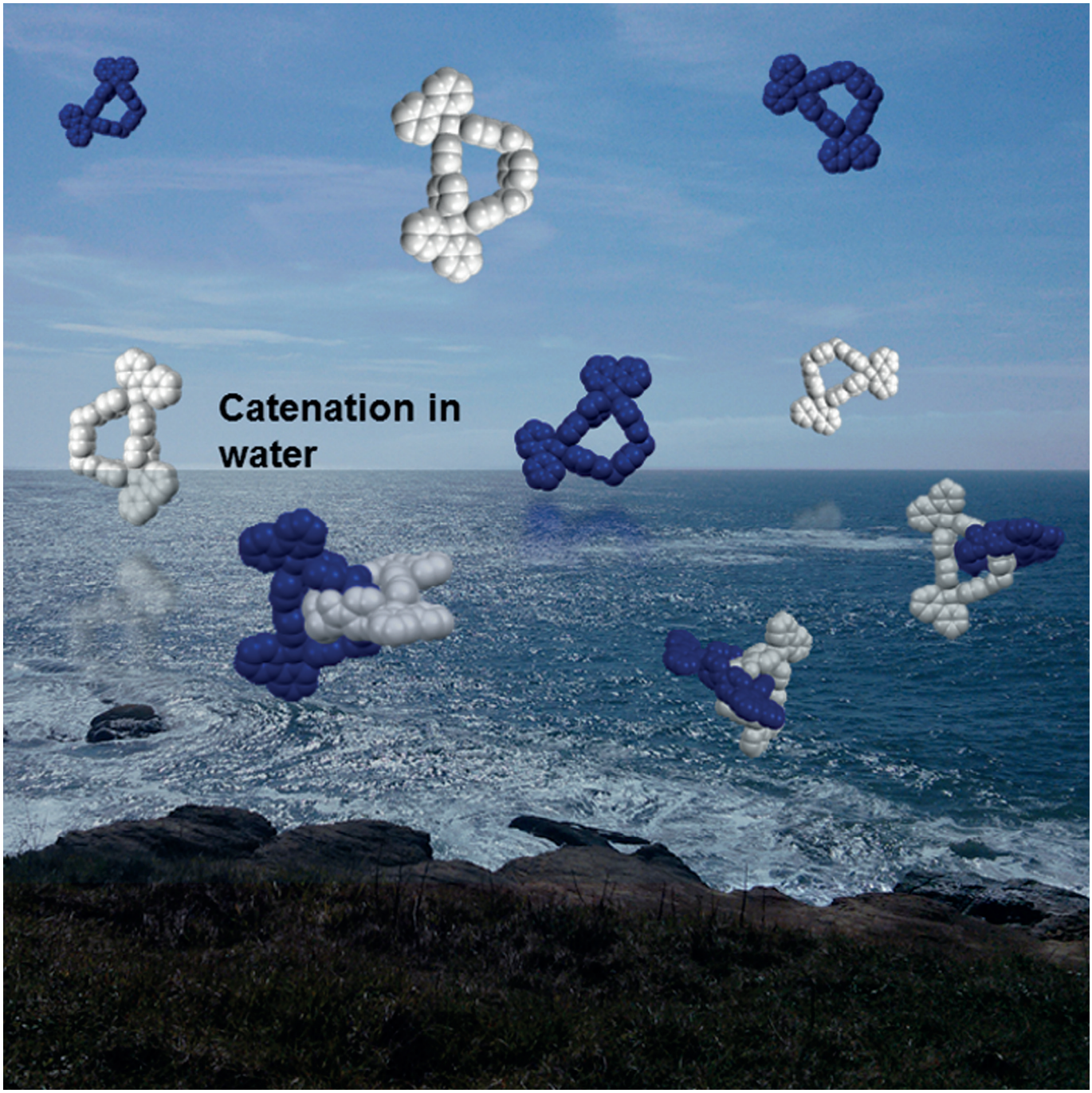

Abstract: Complexation of 1,4-phenylenebis(methylene) diisonicotinate, **L1**, with *cis*-protected Pd^{II} components, $[Pd(\mathbf{L}')(NO_3)_2]$, in an equimolar ratio yielded binuclear complexes, **1a–d** of $[Pd_2(\mathbf{L}')_2(\mathbf{L1})_2](NO_3)_4$ formulation where **L′** stands for ethylenediamine (en), tetramethylethylenediamine (tmeda), 2,2′-bipyridine (bpy), and phenanthroline (phen). The combination of 4,4′-bipyridine, **L2**, with the *cis*-protected Pd^{II} units is known to yield molecular squares, **2a–d**. However, **2b–d** coexist with the corresponding molecular triangles, **3b–d**. Combination of an equivalent each of the ligands **L1** and **L2** with two equivalents of *cis*-protected Pd^{II} components in DMSO resulted in the D-shaped heteroligated complexes $[Pd_2(\mathbf{L}')_2(\mathbf{L1})(\mathbf{L2})](NO_3)_4$, **4a–d**. Two units of the D-shaped complexes interlock, in a concentration dependent fashion, to form the corresponding [2]catenanes $[Pd_2(\mathbf{L}')_2(\mathbf{L1})(\mathbf{L2})]_2(NO_3)_8$, **5a–d** under aqueous conditions. Crystal structures of the macrocycle $[Pd_2(tmeda)_2(\mathbf{L1})(\mathbf{L2})](PF_6)_4$, **4b′′**, and the catenane $[Pd_2(bpy)_2(\mathbf{L1})(\mathbf{L2})]_2(NO_3)_8$, **5c**, provide unequivocal support for the proposed molecular architectures.

Introduction

Mechanically interlocked molecules[1] continue to fascinate chemists owing to the inherent challenges in their synthesis, intriguing structural features, dynamic behavior, and potential applications in the form of molecular machines[2] and sensors.[3] Interlocked molecular species of various topologies, such as catenanes,[4] rotaxanes,[5] knots,[6] Borromean rings,[7] Solomon links[8] and interlocked cages,[9] have been prepared in the laboratory.

The first catenane prepared in the laboratory, more than five decades ago,[10] was a [2]catenane (molecule with Hopf link topology), composed of a pair of interlocked rings and was isolated in a very low yield. The [2]catenanes are particularly attractive because of their potential applications in molecular devices using the controlled gliding motion of the linked rings.[11] The synthesis of a variety of catenanes has been accomplished by using only acyclic components or a mixture of acyclic and macrocyclic components. Both interlocking and cyclization must happen in a cooperative manner during the synthesis to afford the catenanes in high yields. In the cyclization steps, either covalent[4,12a–v] or coordinate-covalent bonds[4,13a–e] are formed, depending upon the component design, where the nature of the cyclization routes are conventional and self-assembly, respectively. Proper orientation of the participating components is essential to assemble the catenane from its components in a targeted manner. The chemical forces responsible for catenation are aromatic donor/acceptor,[12e–f,13a–e] hydrophobic,[13d] hydrogen bonding,[12g–k] and metal(template)–ligand interactions.[12l–p] Anionic[12q–s] and radical templates[12t,u] have also been exploited for synthesizing such interlocked species, in addition to the well-explored metal ion templated synthesis.

The use of a metal ion as part of the catenane rings instead of a template is a convenient strategy, whereupon the cyclization occurs owing to coordinate-covalent bond formation. In this strategy, the rings, that is, the self-assembled metallomacrocycles, are fabricated in situ and subsequently form catenanes. Metallomacrocycles containing Fe^{II}, Ru^{II}, Pd^{II}, Pt^{II}, Cu^{II}, Ag^{I}, Au^{III}, and Zn^{II} have been utilized for the synthesis of a variety of catenanes.[14] Among these metal ions, Pd^{II} has a distinct advantage over others owing to the favorable dynamic behavior of the metal–ligand interaction, which is indispensable for the self-healing of wrongly formed structures. Fujita et al. reported the synthesis of a [2]catenane of general formula $(\mathbf{M_2L'_2L_2})_2$, demonstrating the use of metallomacrocycles in catenane synthesis. The catenane was obtained by combining equimolar amounts of a *cis*-protected Pd^{II} center, **ML′**, and a pyridyl appended bidentate non-chelating ligand, **L**, under aqueous conditions.[15] This catenane is composed of a pair of identical macrocyclic rings, each having a general formula of $\mathbf{M_2L'_2L_2}$, where **L′** is ethylenediamine (en). Although catenanes of a few other formulations have been prepared from *cis*-protected Pd^{II} and suitable ligands, these are limited in number in contrast to the large number of Pd^{II}-based self-assembled coordination complexes that are not interlocked.[16] The comparative shortage of *cis*-protected Pd^{II}-containing catenanes can be ascribed to the difficulty in identifying suitable ligand components for the synthesis of the targeted catenanes.

We are interested in probing the influence of *cis*-protecting agents on different aspects of Pd^{II}-based self-assembled coordination compounds. The focus of our interest so far has been in the fields of crystal engineering,[17] ligand exchange reactions,[18] and one-pot synthesis.[19] In the present work, we have used a variety of *cis*-protected Pd^{II} components, **ML′**, for the construction of metallomacrocycles and [2]catenanes (Figure 1).

The [2]catenanes of general formula $(\mathbf{M_2L'_2(L1)(L2)})_2$ are prepared by the one-pot combination of a mixture of the "flexible" ligand, **L1**, and the "rigid" ligand, **L2**, with a variety of *cis*-protected Pd^{II} components, **ML′**, under appropriate reaction conditions. **L′** stands for ethylenediamine (en), tetramethylethylenediamine (tmeda), 2,2′-bipyridine (bpy), and phenanthro-

[a] *S. Prusty,[+] Dr. S. Krishnaswamy,[+] S. Bandi, Prof. Dr. D. K. Chand*
Department of Chemistry, Indian Institute of Technology Madras
Chennai 600036 (India)
E-mail: dillip@iitm.ac.in

[b] *Dr. B. Chandrika*
Sophisticated Analytical Instrument Facility
Indian Institute of Technology Madras, Chennai 600036 (India)

[c] *Dr. J. Luo, Prof. Dr. G. S. Hanan*
Department of Chemistry, University of Montreal, Montreal (Canada)

[d] *Dr. J. Luo, Prof. Dr. J. S. McIndoe*
Department of Chemistry, University of Victoria, Victoria (Canada)

[+] *These authors contributed equally to this work.*

Supporting information for this article is available on the WWW under http://dx.doi.org/10.1002/chem.201502394.

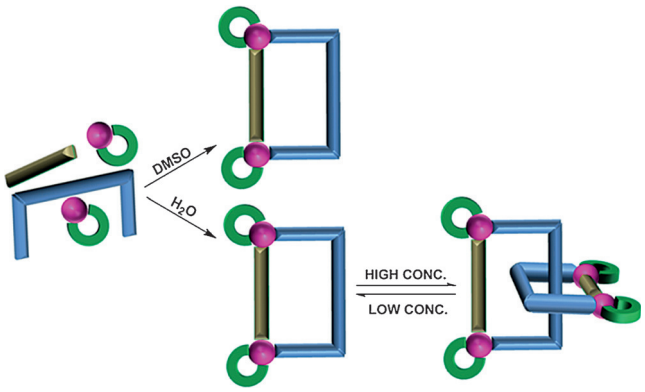

Figure 1. Cartoon representation of the one-pot synthesis of the D-shaped metallomacrocycle $\mathbf{M_2L'_2(L1)(L2)}$ and [2]catenane $(\mathbf{M^2L'_2(L1)(L2)})_2$. The C shape and the rod represent **L1** and **L2**, whereas the semi-protected sphere represents **ML′**. **L′** is en, tmeda, bpy, or phen (**a**–**d**).

line (phen); the other ligands used are 1,4-phenylenebis(methylene) diisonicotinate, **L1**, (Figure 2) and 4,4′-bipyridine, **L2**. A comparable design was reported previously, using **L2** and a rigid ligand in place of **L1**, with en as **L′**. Interestingly, the individual ring was not detected in that design owing to the high stability of the catenane, even at low concentration.[20] In the present study, the individual D-shaped rings of general formula $\mathbf{M_2L'_2(L1)(L2)}$ are prepared by performing the complexation in DMSO (Figure 1). The D-shaped rings can be considered as molecular karabiners bearing coordination-bond gates, in line with the spring gate of real karabiners. The spring or coordination bond is the force responsible for releasing/closing the gate to assist the interlocking phenomenon. The variable concentration dynamic equilibrium of the D-shaped metallomacrocycles with corresponding [2]catenanes (Figure 1) is studied (in D_2O) using ^1H NMR techniques. The diffusion constants determined by DOSY techniques further confirm their solution behavior. The crystal structures of one of the individual D-shaped rings and one of the [2]catenanes provide reliable evidence for the proposed molecular architectures. Preferential formation of the D-shaped rings is supported by DFT calculations.

Results and Discussion

Geometrical description of the ligands and their coordination vectors

The structure and coordination abilities of the ligands **L1** and **L2** is briefly presented here. The well-known compound 4,4′ bipyridine, **L2**, is widely utilized as a ligand for the synthesis of discrete[21] as well as polymeric[22] coordination complexes, owing to its ability to act as a rod-like building block. The directions of the coordination vectors present in **L2** are fixed owing to the rigid nature of the ligand backbone. The rotation of the pyridyl units around the pyridyl–pyridyl bond does not alter the direction of the coordination vectors.

The synthesis of the pyridyl-appended non-chelating bidentate ligand **L1** has been reported in the literature,[23] but it has not been used for the preparation of metallomacrocycles. However, it acts as a linker in some binuclear organometallic[23a] and porphyrin-based Zn^{II} complexes.[23b] The flexibility in **L1** is manifested by the possibility of rotation around phenylene–CH_2, and CH_2–O bonds of the molecule and, to a lesser extent, around the O–C(O) and pyridyl–C(O) bonds. Therefore, the coordination vectors of the ligand **L1** are not located in fixed positions, in contrast to **L2**. Their directions change as a result of the rotations around the above-mentioned bonds. Slow evaporation of a CH_3CN solution of **L1** afforded single crystals suitable for data collection. The crystal structure of uncomplexed **L1** can be used to visualize the direction of its coordination vectors. The compound crystallized in an extended *anti*-conformation (Figure 2a), wherein the coordination vectors of the pyridine rings point in opposite directions (Figure 2b). The planes of the pyridine rings (or isonicotinate moieties) are positioned orthogonal to the plane of the central *p*-phenylene moiety and disposed in an *anti*-fashion. However, in the *syn*-form of **L1** (Figure 2c), the pyridine rings are anticipated to be most suited for the formation of discrete macrocyclic coordination complexes, particularly those of *cis*-protected Pd^{II}. In the *syn*-form, the coordination vectors are expected to be positioned in the same direction, albeit in a somewhat divergent manner. The ligand can easily achieve the *syn*/*anti*-forms through rotation of the substituents around suitable bonds, that is, the phenylene–CH_2 bond(s). Additional rotation around the CH_2–O bonds can shorten the non-bonded distance between the pyridine nitrogen atoms and position the coordination vectors in a less divergent fashion. Thus, the ligand **L1** is capable of adapting to the coordination requirement in a given situation.

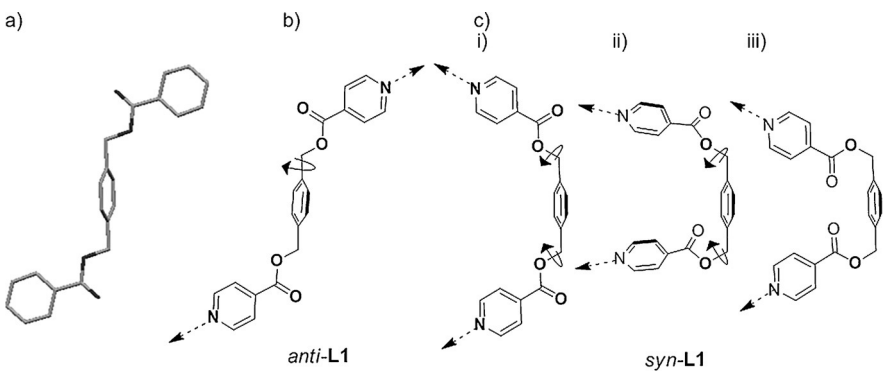

Figure 2. a) Crystal structure of the ligand **L1**; b) and c) Chemical drawing of **L1** showing the *anti* and *syn* conformations.

Complexation of the ligands L1 or L2 with *cis*-protected Pd^{II} components

Complexation of the ligand **L1** with *cis*-protected Pd^{II} components, $[Pd(\mathbf{L}')(NO_3)_2]$ in a 1:1 ratio yielded binuclear complexes, (**1a–d**) of $[Pd_2(\mathbf{L}')_2(\mathbf{L1})_2](NO_3)_4$ formulation, where **L′** represents en (**1a**), tmeda (**1b**), bpy (**1c**), and phen (**1d**) (Scheme 1). Detailed description of the synthesis and characterization of these complexes is given below.

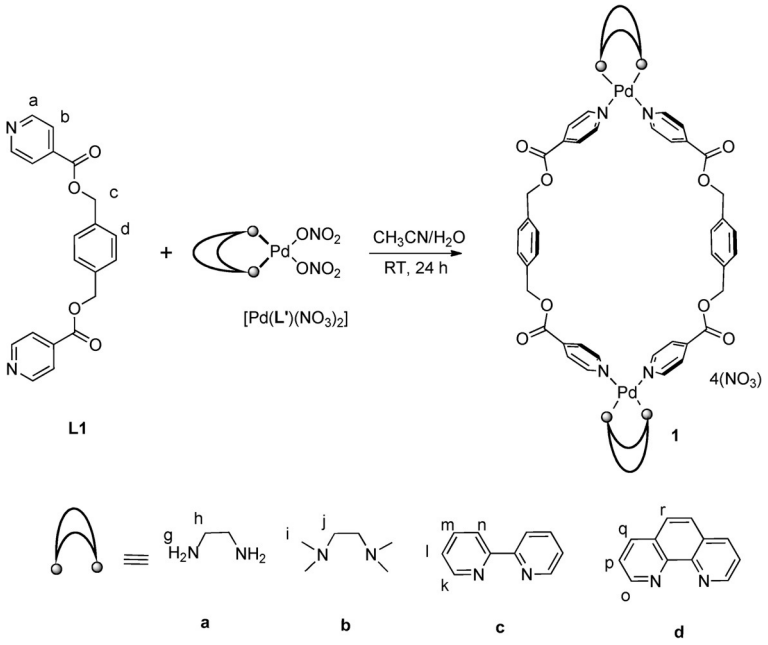

Scheme 1. Synthesis of the metallomacrocycles $[Pd_2(\mathbf{L}')_2(\mathbf{L1})_2](NO_3)_4$, **1a–d**.

The combination of **L2** and $[Pd(en)(NO_3)_2]$ in a 1:1 ratio is known to yield a highly symmetric molecular square-type of complex, that is, $[Pd_4(en)_4(\mathbf{L2})_4](NO_3)_8$, **2a** (Scheme 2).[21a] However, complexation of **L2** with $[Pd(tmeda)(NO_3)_2]$[21b] in a 1:1 ratio results in an equilibrium mixture of molecular square- and molecular triangle-shaped complexes $[Pd_4(tmeda)_4(\mathbf{L2})_4](NO_3)_8$, **2b**, and $[Pd_3(tmeda)_3(\mathbf{L2})_3](NO_3)_6$, **3b** (Scheme 2). Similar equilibria of squares/triangles, that is, **2c**/**3c** or **2d**/**3d** are also obtained when the *cis*-protecting components (**L′**) employed are bpy[21c] or phen,[21d] respectively (Scheme 2).

Combination of equimolar amounts of the ligand **L1** (10 mM) and *cis*-protected Pd^{II} components $[Pd(\mathbf{L}')(NO_3)_2]$ in 1:1 CH_3CN/H_2O at ambient temperature resulted in clear solutions. The solutions were stirred for 24 h and then subjected to slow evaporation to afford the corresponding binuclear complexes **1a–d**. The complexes were characterized by their 1D and 2D NMR spectra in $[D_6]$DMSO (see the Supporting Information, Figures S2–S21). The complexes were also prepared by dissolving the ligand and metal components directly in $[D_6]$DMSO. The NMR spectra of the isolated and in situ prepared complexes are comparable. The complexation reactions were performed in CH_3CN/H_2O (not in DMSO) to facilitate the isolation of complexes. Comparison of the ^{1}H NMR spectra of **1a–d** with that of ligand **L1** revealed a downfield shift of the signals corresponding to the pyridine α and β protons of **L1** (H_a and H_b), attributed to the electron-withdrawing effect of the metal centers. The complexation-induced changes in the chemical shift values for the protons of the ligand moieties in **1a–d** are summarized in Table 1. For instance, in **1b**, the pyridine α protons (H_a) appear at 9.93 ppm, that is, 0.59 ppm downfield relative to the ligand **L1**. The pyridine β protons (H_b) are less influenced by the metal center and are situated at 8.62 ppm, with a downfield shift of only 0.22 ppm. The phenylene protons (H_d) are located at 7.97 ppm, having shifted upfield by 0.09 ppm whereas, the methylene protons (H_c) appear at 5.87 ppm, with upfield shift of 0.07 ppm relative to uncomplexed ligand **L1**. The peaks of the protons present in the *cis*-protecting moieties, that is, en, tmeda, bpy, and phen in **1a–d** are located in the expected positions.[17a–b,25]

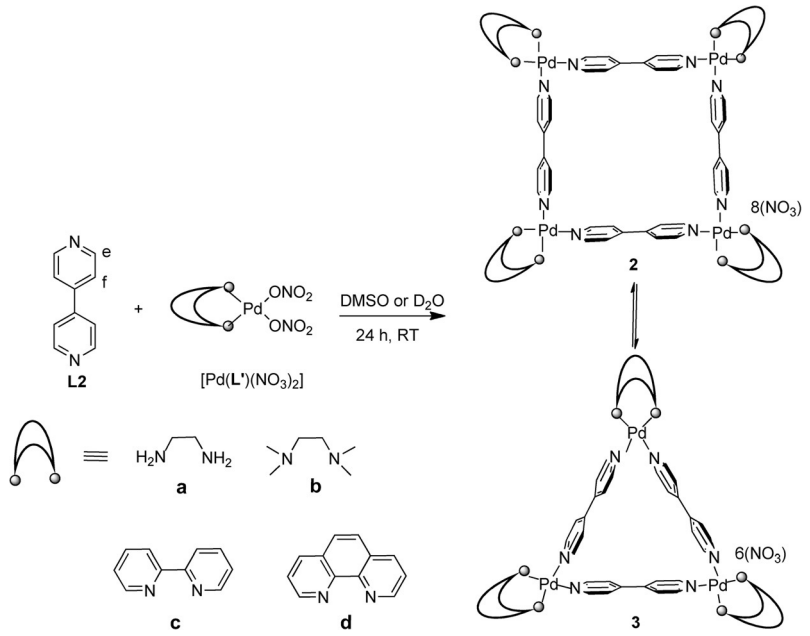

Scheme 2. Synthesis of the molecular square **2a** and the equilibrium mixtures of the molecular square-/triangle-type compounds, that is, **2b/3b**, **2c/3c**, and **2d/3d**. The equilibrium mixture of **2d** and **3d** and their synthesis is previously unpublished,[21d] whereas the other compounds are reported.[21a–c]

The evidence for the formation of these binuclear com-

Table 1. Selected ^{1}H NMR chemical shift data ([D$_6$]DMSO) showing the complexation-induced changes due to formation of the macrocycles **1a–d**.

Complex	$\Delta\delta$ [ppm] (compared with **L1**)			
	H_a	H_b	H_c	H_d
1a	0.15	0.13	−0.05	−0.11
1b	0.59	0.22	−0.07	−0.1
1c	0.71	0.39	0.02	−0.02
1d	0.64	0.36	0.01	−0.03

plexes was gathered from cold-spray ionization mass spectrometry[24a] (CSI-MS) data (see the Supporting Information, Figures S87–S98). The mass spectrum of **1a** showed relevant peaks at $m/z = 577.0713$, which corresponds to the dication [**1a**-2NO$_3$]$^{2+}$. Similarly, the complexes **1b′**, **1c**, and **1d** showed peaks at $m/z = 409.7674$, 1408.1255, and 1456.1257 corresponding to the ions [**1b′**-3BF$_4$]$^{3+}$, [**1c**-(NO$_3$)]$^+$, and [**1d**-(NO$_3$)]$^+$, respectively. The isotopic distributions for these ions are consistent with the theoretically predicted distributions. Other ions are also present in the mass spectra. Coldspray ionization is a very soft ionization method, helping to preserve labile interactions as the ions move from solution to gas phase, but this increases the likelihood of seeing additional signals arising from different charge states due to ion pairing, aggregates, and solvent adducts.[24a,b]

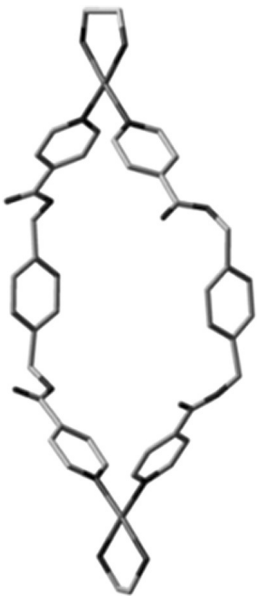

Figure 3. Energy-minimized structure of [Pd$_2$(en)$_2$(**L1**)$_2$]$^{4+}$, that is, the cationic fragment of complex **1a**.

Attempts to grow single crystals of the complexes **1a–d** proved unsuccessful. The energy-minimized structure of the cationic fragment of the complex **1a**, obtained from DFT study using the Gaussian 09 package,[25] is shown in Figure 3 (see the Supporting Information for details). The energy-minimized structure is a good model of the molecular architecture. The conformation of the coordinated ligand in the energy-minimized structure is close to that shown in Figure 2c) ii), resulting in some strain in the molecule, which is relieved by the slight bending of some of the planes to satisfy the square-planar coordination geometry around the Pd^{II} centers.

Complexation of a mixture of the ligands L1 and L2 with *cis*-protected Pd^{II} components in DMSO: D-shaped molecular karabiner like macrocycles, 4a–4d

Combination of an equimolar mixture of the ligand **L1** (5 mM) and **L2** with two equivalents of the *cis*-protected Pd^{II} components [Pd(**L′**)(NO$_3$)$_2$] in DMSO or DMF at ambient temperature resulted in clear solutions. The solutions were stirred for 24 h and the complexes [Pd$_2$(**L′**)$_2$(**L1**)(**L2**)](NO$_3$)$_4$, **4a–d** (Scheme 3) were isolated as off-white solids by precipitation upon addition of excess EtOAc. The complexes were characterized by their

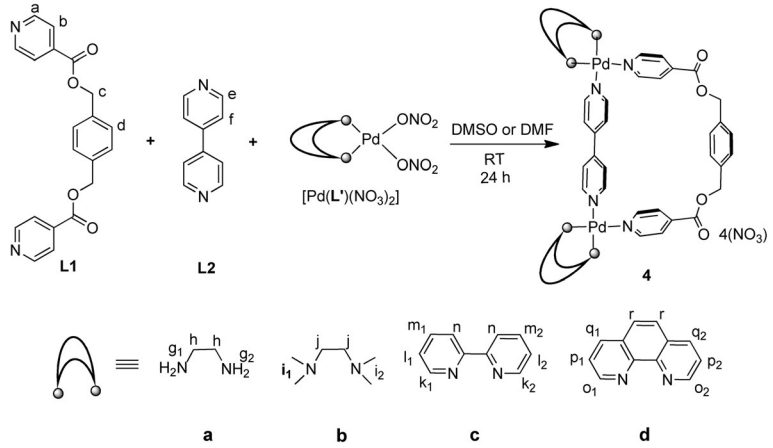

Scheme 3. One-pot synthesis of the D-shaped macrocycles [Pd$_2$(**L′**)$_2$(**L1**)(**L2**)](NO$_3$)$_4$, **4a–d**.

1D and 2D NMR spectra in [D$_6$]DMSO (see the Supporting Information, Figures S22–S43). The complexes were also prepared by dissolving the ligand and metal components directly in [D$_6$]DMSO. A model experiment suggested that synthesis of **4b** is possible in a CH$_3$CN/H$_2$O mixture, but only at low concentration. At higher concentration, a dynamic equilibrium of **4b** with the corresponding [2]catenane is observed (discussed later).

NMR spectra of the isolated and in situ prepared complexes **4a–d** are found to be closely comparable. The ^{1}H NMR spectra of the complexes recorded in [D$_6$]DMSO were compared with those of **L1** and **L2**. The peaks corresponding to the pyridine α and β protons (i.e., H_a, H_b and H_e, H_f) showed downfield shifts. This is ascribed to the electron-withdrawing effect of the metal centers. However, no significant change in the chemical shift was observed for the protons corresponding to the phenylene and methylene groups, which is arguably due to their distance from the metal centers. The signals of protons present in the **L′** moieties showed two sets of peaks in the self-assembled complexes owing to the loss of their plane of symmetry ascribed to the heteroligand coordination. The *cis*-protecting groups in the complexes **4c** and **4d** are composed of aromatic rings (i.e., bpy or phen). The signals corresponding to H_k and H_l in bpy (H_o and H_p in phen) showed upfield shift due to the anisotropic effect of the pyridine rings of the coordinated ligands **L1** and **L2**.[17a–b,26]

Ions matching the composition of the complexes **4a–d** were observed in CSI-MS of the samples (see the Supporting Information, Figures S99–S106). The peaks at $m/z = 481.0550$, 537.1153, 364.0447, and 380.0412 correspond to the ions $[\mathbf{4a}\text{-}2NO_3]^{2+}$, $[\mathbf{4b}\text{-}2NO_3]^{2+}$, $[\mathbf{4c}\text{-}3NO_3]^{3+}$, and $[\mathbf{4d}\text{-}3NO_3]^{3+}$, respectively. A molecule of similar design to that of **4** is reported in literature.[27] Crystal structures of one of the complexes, that is, $[Pd_2(\mathbf{L}')_2(\mathbf{L1})(\mathbf{L2})](PF_6)_4$, **4b**′′, is discussed in a later section. The ^{1}H NMR spectra of the complexes **4b** and **4b**′′ are found to be closely comparable.

Reorganization of 1 and 2/(2+3) into 4 in DMSO

Stock solutions of the preformed complexes of **L1** and **L2**, that is, $[Pd_2(\mathbf{L}')_2(\mathbf{L1})_2](NO_3)_4$ (10 mM in metal) and $[Pd_x(\mathbf{L}')_x(\mathbf{L2})_x](NO_3)_{2x}$ (10 mM in metal) were prepared in [D$_6$]DMSO. Equal volumes of the solutions were combined, where upon reorganization took place and the complexes $[Pd_2(\mathbf{L}')_2(\mathbf{L1})(\mathbf{L2})](NO_3)_4$, **4a–d**, were formed as observed from ^{1}H NMR spectra (see the Supporting Information, Figures S75–S78). One example of the reorganization was monitored by ^{1}H NMR and is described below. When a solution of the macrocycle **1b** was added to a solution containing (**2b**+**3b**), the ^{1}H NMR spectrum showed the appearance of a new set of peaks at the expense of those of **1b**, **2b**, and **3b**. The new set of peaks is assignable to the D-shaped macrocycle **4b**. The conversion occurred rapidly and the peaks corresponding to only **4b** could be seen in approximately 2 h (Figure 4). Similar results were also obtained in the reorganization experiments that targeted the other complexes (**4a**, **4c**, and **4d**). This indicates that the D-shaped macrocycles are probably more stable than the collective stability of the complexes **1** and **2**/**2**+**3**.

The overall free energy and the enthalpy change for the formation of **4a** from **1a** and **2a** are calculated to be -340.778 kcal mol^{-1}, and -335.736 kcal mol^{-1}, respectively (see the Supporting Information, Figure S119, Table S1). The change in entropy was found to be 0.01692 kcal mol^{-1}K^{-1}. These values were obtained by using the Gaussian 09 package.[25] The data indicates the feasibility of formation of the D-shaped complexes through reorganization.

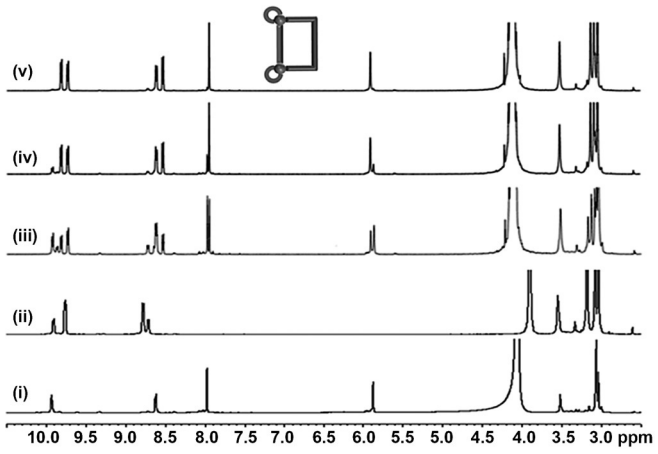

Figure 4. ^{1}H NMR spectra (400 MHz, [D$_6$]DMSO, 25 °C, TMS as an external standard) of: (i) **1b**; (ii) equilibrium mixture of **2b** and **3b**; ^{1}H NMR spectra of a mixture of **1b**, **2b**, and **3b** recorded after (iii) 5 min; (iv) 30 min; and (v) 2 h. After 2 h, complete reorganization occurred to form **4b** as depicted in the ^{1}H NMR spectrum in (v).

From molecular karabiners to [2]catenanes

In anticipation of a possible interlocking of two units of the D-shaped karabiners in aqueous conditions, the ^{1}H NMR spectrum of **4b** (isolated as described above) was recorded in D$_2$O. As expected, two sets of signals were observed (see the Supporting Information, Figure S53). Although one of the sets is attributed to the macrocycle **4b**, the other set clearly exhibited the signature of a [2]catenane, **5b**. Thus, the coordination-bond loaded gate of the karabiners opened and then closed with concomitant interlocking. Detailed description of the catenane formation is provided below.

Complexation of a mixture of the ligands L1 and L2 with *cis*-protected Pd^{II} components in H$_2$O: Dynamic equilibrium of D-shaped macrocycle and corresponding [2]catenane

Combination of an equimolar mixture of the ligand **L1** and **L2** with two equivalents of *cis*-protected Pd^{II} components $[Pd(\mathbf{L}')(NO_3)_2]$, where $\mathbf{L}' =$ en, tmeda, bpy, or phen, in H$_2$O at ambient temperature resulted in clear solutions in 2–8 h. The off-white solids obtained by the evaporation of the reaction mixtures yielded a pair of related complexes, **4a/5a–4d/5d** (Scheme 4). The ^{1}H NMR spectrum of a sample recorded in D$_2$O revealed two sets of signals, attributed to the coexistence of the macrocycle and the [2]catenane, for instance, **4b** and **5b**. The 1D and 2D NMR spectra of the equilibrium mixtures in D$_2$O are provided (see the Supporting Information, Figures S44–S46, S53–S55, S63–S66, S70–S73). One of the equilibria is explained here in detail.

The macrocycle **4b** and the corresponding catenane **5b** exist as equilibrating mixtures of complexes (Figure 5 (iv)). Further, the equilibrium is found to be concentration dependent as discussed in the next section. In one of the sets, the peaks for the phenylene proton, H$_d$, and the methylene proton, H$_c$, of the **L1** moieties are located in the usual positions. However, in the other set, these protons are shifted significantly upfield. This upfield shift is a signature of the interlocking of the rings,[15,20] that is, the formation of the catenanes **5a–d**. These protons in the catenanes are designated as H$_{d'}$ and H$_{c'}$, respectively. The upfield shift of the protons is attributed to the influence of the diatropic ring currents of the five aromatic moieties of one of the interlocked macrocycles on the partner ring and vice versa. In the macrocycle **4b**, the phenylene (H$_d$) and methylene (H$_c$) protons of coordinated ligand **L1** are seen at 7.41 and 5.50 ppm, respectively (Figure 5 (vi)). The insolubility of ligand **L1** in water precluded comparison of its ^{1}H NMR chemical shifts in D$_2$O in the free and complexed forms. However, the peaks for the phenylene and methylene protons (i.e., H$_{d'}$ and H$_{c'}$, respectively) of the coordinated ligand **L1** in the catenane **5b** are observed at 5.08 and 4.58 ppm, respectively (Figure 5 (i)). Thus, a direct comparison of the macrocycles with

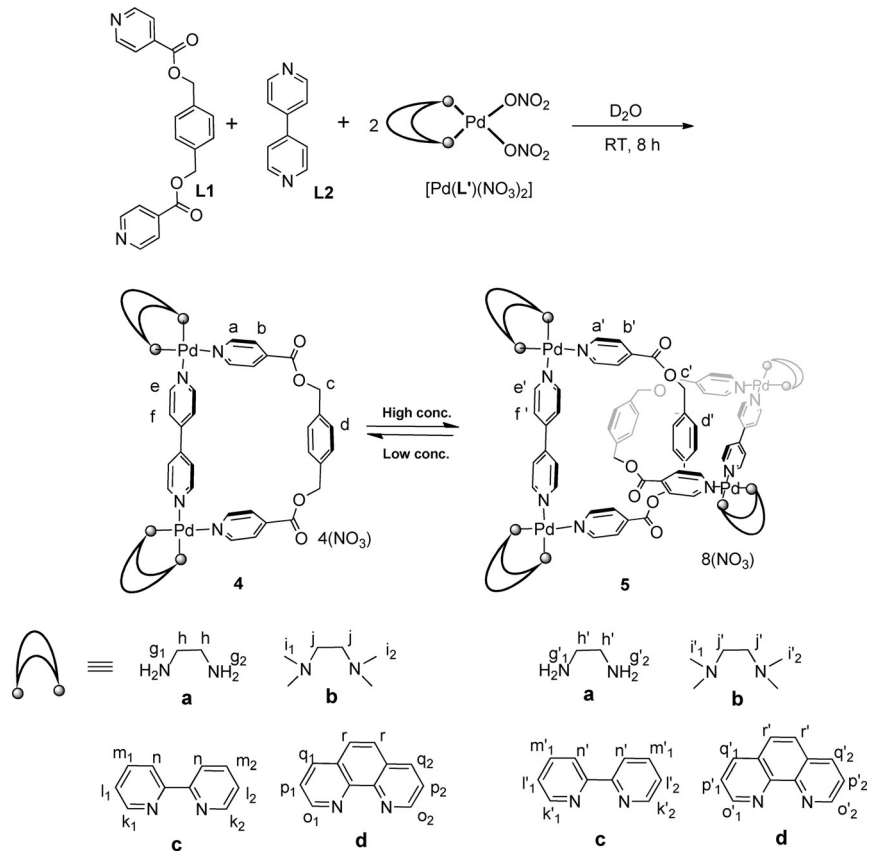

Scheme 4. Synthesis of the complexes **4a–d** and **5a–d**.

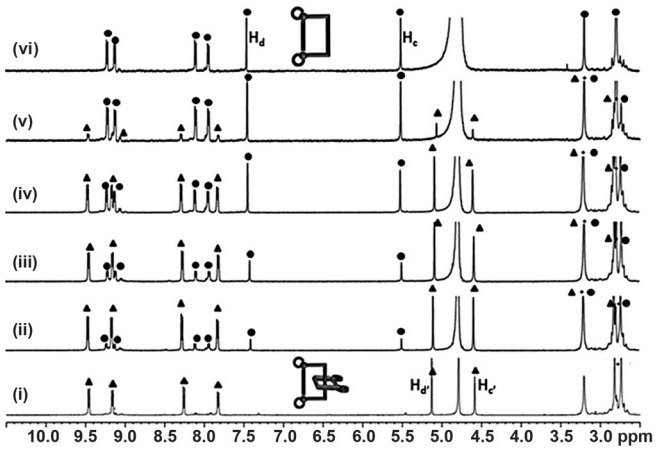

Figure 5. Variable-concentration ^{1}H NMR spectra (400 MHz, D_2O, 25 °C, TMS as an external standard) of (**4b**+**5b**) at: (i) 50; (ii) 15; (iii) 8; (iv) 4; (v) 1; and (vi) 0.25 mM (with respect to Pd^{II}). The circle (●) and triangle (▲) symbols represent the macrocycle, **4b**, and the [2]catenane, **5b**, respectively.

the catenanes is possible. The locations of phenylene as well as methylene protons of macrocycles **4a–d** (H_d and H_c), and that of [2]catenanes **5a–d** ($H_{d'}$ and $H_{c'}$) in the ^{1}H NMR spectra and their differences are summarized in Table 2.

Evidence for [2]catenane formation and the overall compositions was further obtained from CSI-MS and DOSY-NMR studies. The X-ray crystal structure of one of the catenanes provides proof for the proposed architecture and the interlocking. Ions matching the composition of the complexes were detected in the CSI-MS of the samples (see the Supporting Information, Figures S107–118). The mass spectrum of an aqueous solution of **4a**+**5a** revealed peaks at m/z=481.1012 and 661.7941, which could be attributed to the polycations $[\mathbf{4a}\text{-}2NO_3]^{2+}$ and $[\mathbf{5a}\text{-}3NO_3]^{3+}$, respectively. Similarly, the mass spectrum of the mixture **4b′**+**5b′** showed peaks at m/z= 561.6326 and 777.8470, which correspond to the ions $[\mathbf{4b}'\text{-}2BF_4]^{2+}$ and $[\mathbf{5b}'\text{-}3BF_4]^{3+}$, respectively. The concomitant presence of **4c′** and **5c′** was observed in the mass spectrum, which showed peaks at m/z=601.5667 and 831.1043 assignable to $[\mathbf{4c}'\text{-}2BF_4]^{2+}$ and $[\mathbf{5c}'\text{-}3BF_4]^{3+}$, respectively. The mass spectrum for **4d′**+**5d′** showed peaks at m/z=625.5715 and 863.1007, corresponding to $[\mathbf{4d}'\text{-}2BF_4]^{2+}$ and $[\mathbf{5d}'\text{-}3BF_4]^{3+}$, respectively. The isotopic distributions for the peaks of the above-mentioned ions were consistent with the theoretical distributions.

Concentration-dependent equilibrium of macrocycles and [2]catenanes in D_2O

The equilibrium between the D-shaped macrocycles and their corresponding [2]catenanes (**4a**+**5a**, **4b**+**5b**, **4c**+**5c**, and **4d**+**5d**) in D_2O was studied by recording their ^{1}H NMR spectra at different concentrations by successive dilution experiments at ambient temperature in D_2O (see the Supporting Information, Figures S52, S61, S69, S74). At lower concentrations, the D-shaped macrocycles **4a–d** are the exclusive products and at higher concentrations the [2]catenanes **5a**,**b** are found as the exclusive products. Owing to solubility problems, **5c**,**d** could not be prepared exclusively in the solution state. The 1D and 2D NMR spectra of **5a**,**b** in D_2O are provided (see the Supporting Information, Figures S47–S51, S56–S60). The results obtained from the equilibrium mixture of **4b** and **5b** is described here. At lower concentrations, the macrocycle **4b** is the major product, whereas at higher concentrations the equilibrium shifted in favor of the corresponding [2]catenane, **5b** (Figure 5). The complexes containing aliphatic *cis*-protecting groups (en and tmeda) were found to be clearly soluble in water, whereas solubility issues occurred for those containing aromatic *cis*-protecting groups (bpy and phen), particularly at higher concentrations. Hence, a higher percentage of catenane

Table 2. ^{1}H NMR chemical shift data (ppm) for phenylene and methylene protons of the macrocycles **4a–d** and [2]catenanes **5a–d** in D_2O.

Complexes	Phenylene proton H_d of macrocycle	Phenylene proton $H_{d'}$ of [2]catenane	$\Delta\delta$ due to catenane formation	Methylene proton H_c of macrocycle	Methylene proton $H_{c'}$ of [2]catenane	$\Delta\delta$ due to catenane formation
4a/5a	7.35	5.23	−2.12	5.40	4.46	−0.94
4b/5b	7.41	5.08	−2.33	5.50	4.58	−0.92
4c/5c	7.46	5.31	−2.15	5.53	4.66	−0.87
4d/5d	7.49	5.40	−2.09	5.56	4.73	−0.83

was observed in the mixtures of **4a**+**5a** and **4b**+**5b** at a given concentration.

The equilibrium constants were calculated from the ^{1}H NMR data as 1.75×10^{-3} and 3.89×10^{-3} $mmol^{-1}L$ for the equilibria of **4a** with **5a** and **4b** with **5b**, respectively (see the Supporting Information for details, Tables S2–S5). The macrocycles and catenanes are composed of one and two rings, respectively. The calculated amount of the macrocycle and catenane present in the equilibrium mixture of **4b** and **5b**, as obtained from the ^{1}H NMR spectrum of a sample prepared at 50 mM with respect to the Pd^{II} component, is explained below. The calculated percentages of rings that existed as [2]catenane and macrocycle are 93 and 7%, respectively. Thus, the molar ratio of catenane and macrocycle at equilibrium is 46.5:7. As the concentration was reduced, the fraction of the macrocycle increased. At 0.25 mM, the macrocycle **4b** was observed as the sole product. The percentages of the rings present as [2]catenane/macrocycle are plotted as a function of the concentration for all the equilibrium mixtures (Figure 6). The calculated free energy and the enthalpy change for the formation of **5a** from two molecules of **4a** are 416.855 kcal mol^{-1} and 398.199 kcal mol^{-1}, respectively (see the Supporting Information for details). The change in entropy is close to zero (−0.06258 kcal mol^{-1} K^{-1}) in the case of the formation of [2]catenane **5a** from two molecules of **4a**. However, the catenane is stabilized by C–H···O and

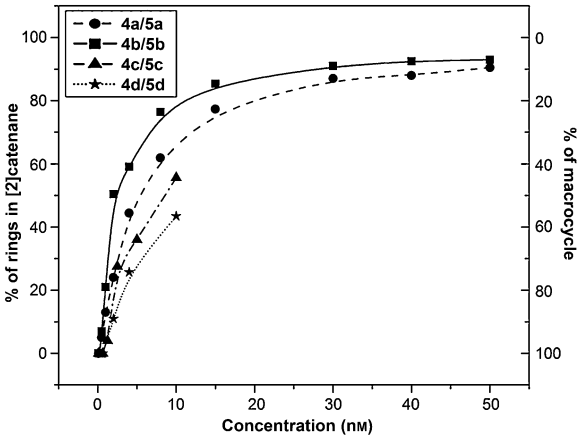

Figure 6. Plot of the percentage of rings in the [2]catenane (**5a–d**) and the macrocycle (**4a–d**) under aqueous conditions, as a function of the concentration. Concentration: with respect to Pd^{II}.

π···π stacking interactions, as suggested by the crystal structure data of the related **5c** (Figure 10). These values were obtained by using the Gaussian 09 package.[25] This suggests that the reaction process is non-spontaneous. However, as per the experimental data, the catenation is found to be feasible at higher concentrations under aqueous conditions.

Influence of acetonitrile on the catenation

To study the effect of solvent on the dynamic equilibrium, CD_3CN was added to a sample of the [2]catenane **5b** in D_2O. Thus, 0.04 mL of CD_3CN was added to 0.4 mL of the sample corresponding to the spectrum shown in Figure 5(i). In this process, immediate reorganization occurred and the proportion of [2]catenane depreciated spontaneously, generating a dynamic equilibrium of **5b** with the D-shaped macrocycle **4b** as observed from its ^{1}H NMR spectrum (see the Supporting Information, Figure S62).

Reorganization of 1 and 2/(2+3) into 4 and 5 in D_2O

Combination of the aqueous solutions of the preformed complexes of **L1**, that is, $[Pd_2(\mathbf{L}')_2(\mathbf{L1})_2](NO_3)_4$, and **L2** (i.e., $[Pd_x(\mathbf{L}')_x(\mathbf{L2})_x](NO_3)_{2x}$), also resulted in reorganization within 8 h. The experiments resulted in the equilibrium mixtures of the D-shaped macrocycles **4a–d** with the corresponding catenanes **5a–d** as observed from ^{1}H NMR spectra (see the Supporting Information, Figures S79–S82) in a comparable proportion as described in the above section.

DOSY NMR study of D-shaped macrocycle and [2]catenane

DOSY (Diffusion Ordered Spectroscopy) NMR is a technique used to detect the presence of multiple species in solution (which diffuse at different rates) and also provides diffusion coefficients.[28] The DOSY NMR spectra for the four sets of equilibrium mixtures (see the Supporting Information, Figures S83–S86) were recorded in D_2O at 25 °C at a concentration where the macrocycle and corresponding [2]catenane are present in approximately equal proportions (determined from variable-concentration ^{1}H NMR data). The dissimilar diffusion rates of the macrocycle and [2]catenane in D_2O enabled the separation of the two components. The macrocycle **4b**, owing to its smaller size, is expected to diffuse faster (diffusion constant = 2.952×10^{-10} m^2s^{-1}) compared with the [2]catenane **5b** (diffusion constant = 2.227×10^{-10} m^2s^{-1}). The DOSY NMR spectra for the equilibrium mixtures **4a**+**5a**, **4b**+**5b**, **4c**+**5c**, and **4d**+**5d** were recorded at concentrations of 8 mM, 2 mM, and 2x5 mM, respectively. The data obtained supports the assignment of the two sets of peaks in the equilibrium mixtures as separate molecules. The bigger molecules correspond to the

peaks assigned for catenane and the smaller to the D-shaped macrocycle. A representative DOSY spectrum of a mixture of **4b** and **5b** is given in Figure 7.

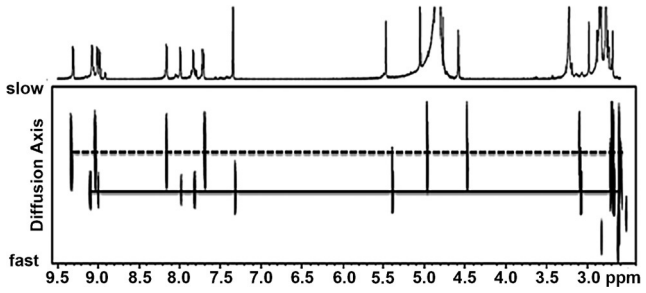

Figure 7. Diffusion-ordered ^{1}H NMR (DOSY) spectrum of a mixture containing **4b** and **5b** in D_2O at 2 mM. The bold line corresponds to macrocycle **4b** and dotted line corresponds to [2]catenane **5b**.

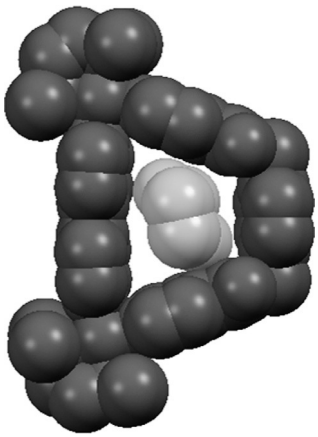

Figure 8. Crystal structure of **4b″** showing inclusion of a 1,4-dioxane molecule. Hydrogen atoms, counter ions, and solvent molecules are omitted for clarity.

Crystallization of D-shaped macrocycles and [2]catenanes

We attempted to crystallize the D-shaped macrocycles **4a–d** and the [2]catenanes **5a–d** using a variety of experiments. As mentioned in the previous sections, the complexes **4** exist in DMSO. However, attempts to crystallize these from their DMSO solutions by slow evaporation, anion exchange, or the vapor diffusion method were unsuccessful. The crystallization experiments were performed by using a mixture of CH_3CN/H_2O as the solvent. However, in this solvent system, **4** exists in equilibrium with **5**. Thus, the cavity of the complex **4** must be occupied to prevent catenation. Keeping this in mind, a set of crystallization experiments were performed targeting the crystals of **4**. Diffusion of solvents such as benzene, toluene, THF, or dioxane were carried out with encapsulation anticipated. The complex $[Pd_2(tmeda)_2(\mathbf{L1})(\mathbf{L2})](PF_6)_4$, **4b″**, crystallized with inclusion of 1,4-dioxane in its cavity. Crystallization of the catenanes **5** was attempted by the method of slow evaporation of their equilibrium mixtures in CH_3CN/H_2O or only H_2O. As the catenanes are favored at higher concentrations, slow evaporation should favor crystallization of **5**. Single crystals of $[Pd_2(bpy)_2(\mathbf{L1})(\mathbf{L2})]_2(NO_3)_4$, **5c**, were obtained by slow evaporation of its solution (in either of the solvent systems). Crystallographic data and structure refinement parameters and ORTEPs corresponding to the crystal structures of **L1**, **4b″**, and **5c** are provided in the Supporting Information (see Table S2 and Figures S120–S123).

Crystal structure of $[Pd_2(tmeda)_2(L1)(L2)](PF_6)_4$·4.5 (1,4-dioxane), 4b″·4.5 (1,4-dioxane)

The complex $[Pd_2(tmeda)_2(\mathbf{L1})(\mathbf{L2})](PF_6)_4$, **4b″**, was synthesized in situ in 1:1 CH_3CN/H_2O. X-ray quality crystals were obtained by diffusing 1,4-dioxane into the solution of **4b″**. The crystals were unstable; hence, they were mounted and analyzed under a liquid nitrogen atmosphere. The macrocycle crystallized in the triclinic space group $P\bar{1}$. A molecule of 1,4-dioxane was found encapsulated in the cavity of the D-shaped molecule (Figure 8).

Crystal structures of [2]catenane $[Pd_2(bpy)_2(L1)(L2)]_2(NO_3)_8$·15 ($H_2O$), 5c·15 ($H_2O$)

Crystals of **5c** suitable for single-crystal X-ray diffraction analysis were obtained by slow evaporation of a 1:1 CH_3CN/H_2O solution of the equilibrium mixture of **4c** and **5c**. The catenane **5c** crystallized in the monoclinic space group *Pc* as a pair of interlocked symmetry-independent molecules. The pair interact in a non-symmetric fashion as observed in the asymmetric unit (Figure 9). The crystals contained a number of water molecules, the slow loss of which resulted in a decrease in crystallinity over time. A total of seven out of eight nitrate anions were located. Catenation of the macrocycles occurs such that the **L2** units are located on the outside; no other isomers were observed. The four metal centers of the rings are disposed in a manner that can be considered as them being located at the corners of a trapezoidal shape. The interlocked rings, arbitrarily designated as macrocycles *A* and *B* (Figure 10), interact through a pair of C–H···O interactions and a number of weak π···π interactions (see the Supporting Information, Table S3).

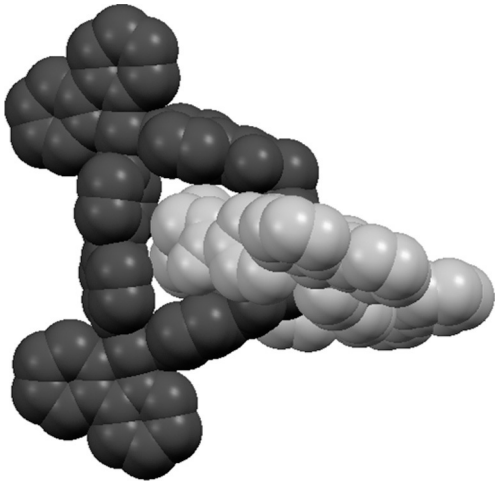

Figure 9. Space-filling view of the asymmetric unit in the crystal structure of **5c**. Hydrogen atoms, anions, and solvent molecules are omitted for clarity.

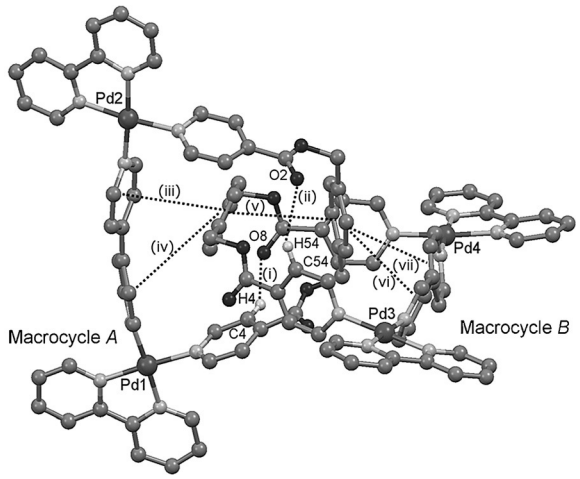

Figure 10. Dotted lines show the C–H···O and π···π interactions between the catenating macrocycles in the crystal structure of **5c**. Hydrogen atoms not involved in hydrogen bonding, disordered solvent, and anions are omitted for clarity.

One of the aromatic protons of the electron-deficient pyridyl aromatic ring of the **L1** moiety of macrocycle *A* is engaged in a short (2.50 Å) and linear (150°) C–H···O interaction (C4–H4···O8) with one of the carbonyl groups of the **L1** moiety of macrocycle *B*. Similarly, the aromatic proton of the electron-deficient pyridyl ring of macrocycle *B* is also involved in a short (2.58 Å) and linear (152°) C–H···O interaction (C54–H54···O2) with the carbonyl oxygen of the **L1** moiety of macrocycle *A* (Figure 10). The interplanar spacing between the aromatic systems, described by the sequence $(4,4'\text{-bpy})_A$-$(\text{phenylene})_B$-$(\text{phenylene})_A$-$(4,4'\text{-bpy})_B$, spans the range 4.65–4.82 Å. However, the planes are not parallel to each other but are tilted with the dihedral angles spanning the range 19.8–44.6°. These separations are larger than those observed in the interlocked rectangular boxes (3.2–3.6 Å).[20]

The N–N non-bonded distances in the **L2** units are in the range of 7.02–7.03 Å in **5c** (7.06 Å in **4b**″) compared with a value of 7.1 Å observed in its own crystals,[29] suggesting that the 4,4′-bpy units are gently bent to accommodate the square-planar coordination geometry around the metal centers. The N–N non-bonded distances in the **L1** units are in the range of 10.11–10.17 Å in **5c** (10.08 Å in **4b**″). The experimental and simulated powder XRD patterns recorded for the crystals of **5c** are found to be comparable, indicating the bulk sample is the catenane (see the Supporting Information, Figure S124).

Conclusion

A series of D-shaped heteroligated complexes of general formula $\mathbf{M_2L'_2(L1)(L2)}$ were prepared. Two units of the D-shaped complexes are interlocked, in a concentration-dependent fashion, to form the corresponding [2]catenanes of $\mathbf{M_2L'_2(L1)(L2)}$ formulation under aqueous conditions. The nature of the solvent, and also the concentration, largely controls the dynamic equilibrium of the D-shaped macrocycle versus the [2]catenanes. The *cis*-protecting moiety **L′** influenced the solubility and crystallinity of the compounds. The interlocked rings are stabilized by a number of C–H···O, and π···π interactions as observed in the solid state.

Experimental Section

Ligand **L1** was prepared by following a literature procedure.[23] The ligand **L2**, $PdCl_2$, and silver salts were acquired from Aldrich, whereas all common reagents and solvents were obtained from Spectrochem, India. The *cis*-protected Pd^{II} units, that is, $Pd(\mathbf{L'})Cl_2$ and $[Pd(\mathbf{L'})(NO_3)_2]$,[30] were synthesized according to literature procedures. The compounds $Pd(\mathbf{L'})(BF_4)_2$ and $Pd(\mathbf{L'})(PF_6)_2$ were prepared by reacting $Pd(\mathbf{L'})Cl_2$ with $AgBF_4$ and $AgPF_6$, respectively. Deuterated solvents $[D]_6DMSO$, CD_3CN, and D_2O were obtained from Aldrich and Cambridge Isotope Laboratories. NMR spectra were recorded with Bruker 400 MHz and 500 MHz FT-NMR spectrometers using tetramethylsilane in $CDCl_3$ as an external reference. The mass spectra were recorded by using a Bruker ESI-TOF/ESI-TRAP/FTMS fitted with a Bruker Cryospray system. Powder XRD patterns were recorded on a Bruker D8 Advance X-ray diffractometer using $Cu_{K\alpha}$ radiation ($\lambda = 1.54178$ Å).

DOSY

Diffusion Ordered Spectroscopy (DOSY) NMR measurements were performed with a Bruker Avance (AV III) 500 MHz NMR spectrometer, equipped with a 5 mm broadband observe (BBO) *z*-axis gradient probe, which delivers a maximum gradient strength of 50 G cm^{-1}. Experiments were carried out with active temperature regulation at 298 K. Self-diffusion coefficients were measured by using the stimulated echo, bipolar gradient (stebpgp1s) pulse sequence. Generally, the diffusion coefficient (*D*) is experimentally determined by monitoring the signal intensity decay in a 1D pulsed-field gradient spin-echo experiment (PFGSE) spectrum as a function of the applied gradient strength.[31] In the two dimensional DOSY experiment,[32–33] the decay of magnetization as a function of increasing gradient intensity (i.e., the gradient ramp) is observed. The gradient ramp in our experiment was adjusted between 2 and 95% strength of the gradient amplifier using 16 equidistant steps. Each experiment was acquired with a spectral width of 4500 Hz and 16k complex points. The diffusion time (Δ) of 100 ms was used and the duration of the gradient pulse (δ) was 1 ms. After Fourier transformation and baseline correction, the spectra were processed with DOSY processing tools from the Bruker Topspin 2.1 package. Data were analyzed by using the variable gradient fitting routines, and in all cases the proton resonances were fit with a single exponential decay function using peak intensities. The diffusion coefficient values reported are an average value obtained based on intensities measured from a minimum of three or four separate peaks.

Crystallography

Single-crystal X-ray measurements were recorded for crystals of **L1**, **4b**″, and **5c** with a Bruker AXS Kappa Apex II CCD diffractometer with graphite-monochromatized ($Mo_{K\alpha}$ $\lambda = 0.71073$ Å) radiation. The crystals were fixed at the tip of a glass fiber, mounted on the goniometer head, and optically centered. The crystals of **4b**″ started cracking when taken out of the sample vial. Hence, one of them was carefully coated with paraffin oil and immediately transferred to the goniometer under a flow of liquid nitrogen (100 K). The automatic cell determination routine, with 36 frames at three different orientations of the detector, was employed to collect re-

flections, and the APEXII-SAINT program[34] was used for determining the unit cell parameters. The data were corrected for Lorentz-polarization effects. Semi-empirical absorption correction (multi-scan) based on symmetry equivalent reflections was applied by using the SADABS program.[35] The structures were solved by direct methods and refined by full-matrix least-squares, based on F^2 by using the SHELX-2014 software package[36] and the program WinGX.[37] All the hydrogen atoms were placed in geometrically idealized positions and refined isotropically. Molecular and packing diagrams were generated using Mercury CSD 3.3/3.5.[38] Geometrical calculations were performed using PLATON.[39]

General procedure A (synthesis of the complexes 1)

Ligand **L1** (0.029 mmol) and the chosen *cis*-protected Pd^{II} unit (0.029 mmol) were added to acetonitrile/water (1:1, 3 mL) and stirred for 24 h at ambient temperature to obtain clear solutions. Slow evaporation of the solutions yielded pale-yellow solid samples. The complexes were also prepared in situ by combining Ligand **L1** (1 equiv) and the corresponding *cis*-protected Pd^{II} unit (1 equiv) in $[D]_6$DMSO (0.6 mL).

$[Pd_2(en)_2(L1)_2](NO_3)_4$, 1a: The complex was synthesized according to general procedure A using **L1** (10.4 mg, 0.029 mmol, 1 equiv) and $Pd(en)(NO_3)_2$ (8.7 mg, 0.029 mmol, 1 equiv). Yield: 15.3 mg, 80%.; m.p.: 218 °C (decomposed); ^{1}H NMR (500 MHz, [D$_6$]DMSO): $\delta = 9.49$ (d, $J = 6.6$ Hz, 8H, H$_a$), 8.54 (d, $J = 6.8$ Hz, 8H, H$_b$), 7.96 (s, 8H, H$_d$), 6.14 (s, 8H, H$_h$), 5.89 (s, 8H, H$_c$), 3.21 ppm (s, 8H, H$_g$); ^{13}C NMR (125 MHz, [D$_6$]DMSO): $\delta = 163.98$, 153.74, 140.74, 136.16, 128.94, 126.23, 68.18, 46.71 ppm; MS (CSI): *m/z* calcd for [**1a**-2NO$_3$]$^{2+}$: 577.0717; found: 577.0713.

$[Pd_2(tmeda)_2(L1)_2](NO_3)_4$, 1b: The complex was synthesized according to general procedure A using **L1** (10.4 mg, 0.029 mmol, 1 equiv) and $Pd(tmeda)(NO_3)_2$ (10.3 mg, 0.029 mmol, 1 equiv). Yield: 17. 2 mg, 83%; m.p.: 212 °C (decomposed); ^{1}H NMR (500 MHz, [D$_6$]DMSO): $\delta = 9.93$ (d, $J = 5.3$ Hz, 8H, H$_a$), 8.62 (d, $J = 8.6$ Hz, 8H, H$_b$), 7.97 (s, 8H, H$_d$), 5.87 (s, 8H, H$_c$), 3.51 (s, 8H, H$_j$), 3.06 ppm (s, 24H, H$_j$); ^{13}C NMR (125 MHz, [D$_6$]DMSO): $\delta = 163.64$, 153.08, 140.49, 135.86, 128.75, 126.78, 68.02, 62.97, 50.98 ppm; MS (CSI): *m/z* calcd for [**1b**′-3BF$_4$]$^{3+}$: 409.7654; found: 409.7674.

Complex **1b′** was prepared in a similar manner by using $Pd(tmeda)(BF_4)_2$ instead of $Pd(tmeda)(NO_3)_2$.

$[Pd_2(bpy)_2(L1)_2](NO_3)_4$, 1c: The complex was synthesized according to general procedure A using **L1** (10.4 mg, 0.029 mmol, 1 equiv) and $Pd(bpy)(NO_3)_2$ (11.5 mg, 0.029 mmol, 1 equiv). Yield: 18.4 mg, 84.01%; m.p.: 222 °C (decomposed); ^{1}H NMR (500 MHz, [D$_6$]DMSO): $\delta = 10.05$ (d, $J = 5.0$ Hz, 8H, H$_a$), 9.64 (d, $J = 8.0$ Hz, 4H, H$_m$), 8.96 (s, 4H, H$_n$), 8.79(d, $J = 5.2$ Hz, 8H, H$_b$), 8.49-8.52 (m, 8H, H$_k$ and H$_l$), 8.04 (s, 8H, H$_d$), 5.97 ppm (s, 8H, H$_c$); ^{13}C NMR (125 MHz, [D$_6$]DMSO): $\delta = 163.45$, 153.40, 151.73, 146.41, 142.08, 141.01, 135.71, 131.08, 129.01, 128.58, 127.26, 67.88 ppm; MS (CSI): *m/z* calcd for [**1c**-(NO$_3$)]$^+$: 1408.1323; found: 1408.1255.

$[Pd_2(phen)_2(L1)_2](NO_3)_4$, 1d: The complex was synthesized according to general procedure A using **L1** (10.4 mg, 0.029 mmol, 1 equiv) and $Pd(phen)(NO_3)_2$ (12.3 mg, 0.029 mmol, 1 equiv). Yield: 19.1 mg, 84.14%; m.p.: 226 °C (decomposed); ^{1}H NMR (500 MHz, [D$_6$]DMSO): $\delta = 9.99$ (s, 8H, H$_a$), 9.30 (d, $J = 8.0$ Hz, 4H, H$_q$), 9.03 (d, $J = 7.8$ Hz, 4H, H$_p$), 8.76 (s, 8H, H$_b$), 8.21 (s, 4H, H$_o$), 8.03 (s, 12H, H$_{r+d}$), 5.95 ppm (s, 8H, H$_c$); ^{13}C NMR (125 MHz, [D$_6$]DMSO): $\delta =$ 163.48, 156.33, 153.19, 150.84, 143.40, 140.96, 135.75, 129.15, 129.04, 128.65, 127.36, 125.20, 67.93 ppm; MS (CSI): *m/z* calcd for [**1d**-(NO$_3$)]$^+$: 1456.1328; found: 1456.1257.

General procedure B (synthesis of the complexes 4)

Ligand **L1** (0.005 mmol), **L2** (0.005 mmol), and the corresponding *cis*-protected Pd^{II} unit (2 equiv) were added to DMSO or DMF (3 mL) and stirred for 24 h at ambient temperature to obtain a clear yellow solution. Addition of excess EtOAc, in a typical isolation process in a given experiment, gave an off-white precipitate, which was separated by filtration, washed several times with EtOAc, and dried under vacuum to obtained an off-white solid. All complexes were isolated in the same fashion.

$[Pd_2(en)_2(L1)(L2)](NO_3)_4$, 4a: The complex was synthesized according to general procedure B (in DMF) using **L1** (1.8 mg, 0.005 mmol), **L2** (0.8 mg, 0.005 mmol), and $Pd(en)(NO_3)_2$ (3.0 mg, 0.010 mmol). Yield: 48.66 mg, 87.5%; m.p.: 218 °C (decomposed); ^{1}H NMR (500 MHz, [D$_6$]DMSO): $\delta = 9.36$ (d, $J = 6.0$ Hz, 8H, H$_a$ and H$_e$), 8.44 and 8.40 (d and d, $J = 6.6$ and 6.1 Hz, 4H and 4H, H$_b$ and H$_f$), 7.91 (s, 4H, H$_d$), 6.14 and 6.10 (s and s, 4H and 4H, H$_{g1}$ and H$_{g2}$), 5.85 (s, 4H, H$_c$), 3.23 ppm (s, 8H, H$_h$); ^{13}C NMR (125 MHz, [D$_6$]DMSO): $\delta = 164.11$, 153.65, 153.26, 146.33, 141.15, 136.87, 130.95, 126.47, 125.11, 68.29, 47.99, 46.98 ppm; MS (CSI): *m/z* calcd for [**4a**-2(NO$_3$)]$^{2+}$: 481.0503; found: 481.0550.

$[Pd_2(tmeda)_2(L1)(L2)](NO_3)_4$, 4b: The complex was synthesized according to general procedure B (in DMF) using **L1** (1.8 mg, 0.005 mmol, 1 equiv), **L2** (0.8 mg, 0.005 mmol, 1 equiv), and $Pd(tmeda)(NO_3)_2$ (3.5 mg, 0.010 mmol, 2 equiv). Yield: 53.61 mg, 87.3%; m.p.: 214 °C (decomposed); ^{1}H NMR (500 MHz, [D$_6$]DMSO): $\delta = 9.84$ and 9.76 (dd and d, $J = 6.5$, 4.0, and 6.7 Hz, 4H and 4H, H$_a$ and H$_e$), 8.67 and 8.56 (d and dd, $J = 6.8$ and 7.0, 4.0 Hz, 4H and 4H, H$_b$ and H$_f$), 7.95 (s, 4H, H$_d$), 5.92 (s, 4H, H$_c$), 3.53 (s, 8H, H$_j$), 3.14 and 3.09 ppm (s and s, 12H and 12H, H$_{i1}$ and H$_{i2}$); ^{13}C NMR (125 MHz, [D$_6$]DMSO): $\delta = 163.27$, 152.75, 152.15, 145.01, 140.09, 136.42, 130.26, 126.49, 124.79, 67.36, 62.75, 50.89, 50.76 ppm; MS (CSI): *m/z* calcd for [**4b**-2(NO$_3$)]$^{2+}$: 537.1131; found: 537.1153.

The complex **4b″** was prepared in a similar manner by using $Pd(tmeda)(PF_6)_2$ instead of $Pd(tmeda)(NO_3)_2$.

$[Pd_2(bpy)_2(L1)(L2)](NO_3)_4$, 4c: The complex was synthesized according to general procedure B (in DMSO or DMF) using combining **L1** (1.8 mg, 0.005 mmol, 1 equiv), **L2** (0.8 mg, 0.005 mmol, 1 equiv), and $Pd(bpy)(NO_3)_2$ (4.0 mg, 0.010 mmol, 2 equiv). Yield: 6.03 mg, 92.1%; m.p.: 222 °C (decomposed); ^{1}H NMR (500 MHz, [D$_6$]DMSO): $\delta = 9.91$ and 9.87 (d and d, $J = 6.6$ and 6.7 Hz, 4H and 4H, H$_a$ and H$_e$), 9.34 (d, $J = 8.0$ Hz, 4H, H$_n$), 9.04–9.08 (m, 4H, H$_{m1+m2}$), 8.80 and 8.67 (d and d, $J = 6.8$ and 6.6 Hz, 4H and 4H, H$_b$ and H$_f$), 8.35 and 8.21 (d and d, $J = 5.5$ and 5.0 Hz, 2H and 2H, H$_{k1}$ and H$_{k2}$), 8.29–8.22 (m, 4H, H$_{l1+l2}$), 8.01 (s, 4H, H$_d$), 5.98 ppm (s, 4H, H$_c$); ^{13}C NMR (125 MHz, [D$_6$]DMSO): $\delta = 163.33$, 156.27, 153.04, 152.50, 151.26, 151.15, 145.93, 143.36, 140.80, 136.40, 130.42, 129.18, 127.23, 125.64, 125.19, 67.55 ppm; MS (CSI): *m/z* calcd for [**4c**-3(NO$_3$)]$^{3+}$: 364.0376; found: 364.0447.

$[Pd_2(phen)_2(L1)(L2)](NO_3)_4$, 4d: The complex was synthesized according to general procedure B (in DMSO or DMF) using combining **L1** (1.8 mg, 0.005 mmol, 1 equiv), **L2** (0.8 mg, 0.005 mmol, 1 equiv), and $Pd(phen)(NO_3)_2$ (4.2 mg, 0.010 mmol, 2 equiv). Yield: 6.54 mg, 96.2%; m.p.: 220 °C (decomposed); ^{1}H NMR (500 MHz, [D$_6$]DMSO): $\delta = 9.98$ and 9.96 (d and d, $J = 6.5$ and 6.5 Hz, 4H and 4H, H$_a$ and H$_e$), 9.70 and 9.69 (dd and dd, $J = 7.8$, 5.0 and 8.0,

5.0 Hz, 2H and 2H, H_{q1} and H_{q2}), 9.00 (s, 4H, H_r), 8.87 and 8.72 (d and d, J=6.5 and 6.5 Hz, 4H and 4H, H_e and H_f), 8.84 and 8.69 (d and d, J=5.3 and 5.3 Hz, 2H and 2H, H_{o1} and H_{o2}), 8.61 and 8.58 (dd and dd, J=8.0, 5.5 and 8.5, 5.5 Hz, 2H and 2H, H_{p1} and H_{p2}), 8.03 (s, 4H, H_d), 6.00 ppm (s, 4H, H_c); ^{13}C NMR (125 MHz, [D$_6$]DMSO): δ=163.40, 153.34, 152.83, 152.35, 152.18, 146.09, 142.18, 142.14, 140.92, 136.42, 131.14, 130.44, 128.73, 127.46, 127.24, 125.70, 67.6 ppm; MS (CSI): *m/z* calcd for [**4d**-3(NO$_3$)]$^{3+}$: 380.0377; found: 380.0412.

General procedure C (synthesis of equilibrium mixture of complexes 4 and 5)

Ligand **L1** (0.025 mmol), **L2** (0.025 mmol) and the corresponding *cis*-protected Pd^{II} unit (0.050 mmol) were mixed in 5 mL water and stirred for 24 h at ambient temperature to obtain a clear solution, which, upon slow evaporation, yielded a pale yellow solid/crystals. When solid was dissolved in D$_2$O, two sets of signals were revealed, corresponding to the macrocycle (**4a**–**d**) and [2]catenane (**5a**–**d**).

[Pd$_2$(en)$_2$(L1)(L2)](NO$_3$)$_4$, 4a, and [Pd$_4$(en)$_4$(L1)$_2$(L2)$_2$](NO$_3$)$_8$, 5a: The equilibrium mixture was synthesized according to general procedure C using **L1** (8.7 mg, 0.025 mmol, 1 equiv), **L2** (3.9 mg, 0.025 mmol, 1 equiv), and Pd(en)(NO$_3$)$_2$ (14.5 mg, 0.050 mmol, 2 equiv). Yield: 24 mg, 88.56%; ^{13}C NMR (125 MHz, D$_2$O): δ=163.47, 152.76, 152.25, 145.48, 140.68, 134.19, 128.26, 126.42, 124.21, 66.56, 47.09 ppm.

*Complex **4a***: ^{1}H NMR (500 MHz, D$_2$O): δ=8.84 (t, J=6.0 Hz, 8H, H_a and H_e), 8.00 and 7.87 (d and d, J=6.5 and 5.9 Hz, 4H and 4H, H_b and H_f), 7.46 (s, 4H, H_d), 5.50 (s, 4H, H_c), 2.98 ppm (s, 24H, H_h); MS (CSI): *m/z* calcd for [**4a**-2(NO$_3$)]$^{2+}$: 481.0503; found: 481.1012.

*Complex **5a***: ^{1}H NMR (500 MHz, D$_2$O): δ=9.18 and 8.92 (d and d, J=6.5 and 6.3 Hz, 8H and 8H, $H_{a'}$ and $H_{e'}$), 7.97 and 7.63 (d and d, J=5.9 and 6.4 Hz, 8H and 8H, $H_{b'}$ and H_f), 5.29 (s, 8H, $H_{d'}$), 4.48 (s, 8H, $H_{c'}$), 2.93 ppm (s, 24H, $H_{h'}$ and H_h); MS (CSI): *m/z* calcd for [**5a**-3(NO$_3$)]$^{3+}$: 661.7303; found: 661.7941.

[Pd$_2$(tmeda)$_2$(L1)(L2)](NO$_3$)$_4$, 4b, and [Pd$_4$(tmeda)$_4$(L1)$_2$(L2)$_2$](NO$_3$)$_8$, 5b: The equilibrium mixture was synthesized according to general procedure C using **L1** (8.7 mg, 0.025 mmol, 1 equiv), **L2** (3.9 mg, 0.025 mmol, 1 equiv), and Pd(tmeda)(NO$_3$)$_2$ (17.3 mg, 0.050 mmol, 2 equiv). Yield: 27 mg, 90.3%; ^{13}C NMR (125 MHz, D$_2$O): δ=163.29, 152.52, 151.96, 144.84, 141.23, 134.04, 128.42, 127.45, 124.51, 66.59, 63.09, 50.68, 50.62 ppm.

*Complex **4b***: ^{1}H NMR (500 MHz, D$_2$O): δ=9.21 and 9.10 (d and d, J=6.4 and 6.6 Hz, 4H and 4H, H_a and H_e), 8.10 and 7.92 (d and d, J=6.6 and 6.6 Hz, 4H and 4H, H_b and H_f), 7.41 (s, 4H, H_d), 5.50 (s, 4H, H_c), 3.19 (s, 24H, $H_{j+j'}$), 2.80 (s, 36H, $H_{i1+i'1}$), 2.66 ppm (s, 36H, $H_{i'2+i2}$); MS (CSI): *m/z* calcd for [**4b**′-2(BF$_4$)]$^{2+}$: 561.6292; found: 561.6326.

*Complex **5b***: ^{1}H NMR (500 MHz, D$_2$O): δ=9.41 and 9.11 (d and d, J=6.6 and 6.5 Hz, 8H and 8H, $H_{a'}$ and $H_{e'}$), 8.21 and 7.76 (d and d, J=6.6 and 6.7 Hz, 8H and 8H, $H_{b'}$ and H_f), 5.07 (s, 8H, $H_{d'}$), 4.53 (s, 8H, $H_{c'}$), 3.15 (s, 24H, $H_{j'+}H_j$), 2.76 (s, 36H, $H_{i'1+}H_{i1}$), 2.68 ppm (s, 36H, $H_{i'2+}H_{i2}$); MS (CSI): *m/z* calcd for [**5b**′-3BF$_4$]$^{3+}$: 777.8403; found: 777.8470.

The mixture of **4b**′ and **5b**′ was prepared in a similar manner by using Pd(tmeda)(BF$_4$)$_2$ instead of Pd(tmeda)(NO$_3$)$_2$.

[Pd$_4$(bpy)$_4$(L1)$_2$(L2)$_2$](NO$_3$)$_8$, 4c, and [Pd$_2$(bpy)$_2$(L1)(L2)](NO$_3$)$_4$, 5c: The equilibrium mixture was synthesized according to general procedure C using **L1** (8.7 mg, 0.025 mmol, 1 equiv), **L2** (3.9 mg, 0.025 mmol, 1 equiv), and Pd(bpy)(NO$_3$)$_2$ (19.3 mg, 0.050 mmol, 2 equiv). Yield: 26.5 mg, 83.1%; ^{13}C NMR (125 MHz, D$_2$O): δ=163.40, 152.98, 152.44, 150.34, 145.80, 143.13, 141.75, 134.23, 128.90, 128.64, 128.29, 127.85, 125.31, 124.65, 66.74 ppm.

*Complex **4c***: ^{1}H NMR (500 MHz, D$_2$O): δ=9.25 and 9.19 (d and d, J=5.95 and 5.95 Hz, 4H and 4H, H_a and H_e), 8.48 (s, 4H, H_n), 8.41–8.36 (m, 12H, $H_{m+}H_{m'}$), 8.16 and 8.06 (d and d, J=6.5 and 6.5 Hz, 4H and 4H, H_b and H_f), 7.65 (t, J=6.0 Hz, 4H, H_l), 7.44 (s, 4H, H_d), 7.65–7.57 (m, 20H, $H_{k+l'+k'}$), 5.51 ppm (s, 4H, H_c); MS (CSI): *m/z* calcd for [**4c**′-2(BF$_4$)]$^{2+}$: 601.5735; found: 601.5667.

*Complex **5c***: ^{1}H NMR (500 MHz, D$_2$O): δ=9.57 and 9.29 (d and d, J=5.95 and 5.95 Hz, 8H and 8H, $H_{a'}$ and $H_{e'}$), 8.50 (s, 8H, $H_{n'}$), 8.41–8.36 (m, 12H, $H_{m'+}H_m$), 8.35 and 8.06 (d and d, J=5.8 and 5.8 Hz, 8H and 8H, $H_{b'}$ and H_f), 7.65–7.57 (m, 20H, $H_{k'+}H_{l'+}H_k$), 5.28 (s, 8H, $H_{d'}$), 4.64 ppm (s, 8H, $H_{c'}$); MS (CSI): *m/z* calcd for [**5c**′-3BF$_4$]$^{3+}$: 831.0904; found: 831.1043.

The mixture of **4c**′ and **5c**′ was prepared in a similar manner by using Pd(bpy)(BF$_4$)$_2$ instead of Pd(bpy)(NO$_3$)$_2$.

[Pd$_2$(phen)$_2$(L1)(L2)](NO$_3$)$_4$, 4d, and [Pd$_4$(phen)$_4$(L1)$_2$(L2)$_2$](NO$_3$)$_8$, 5d: The equilibrium mixture was synthesized according to general procedure C using **L1** (8.7 mg, 0.025 mmol, 1 equiv), **L2** (3.9 mg, 0.025 mmol, 1 equiv), and Pd(phen)(NO$_3$)$_2$ (20.5 mg, 0.050 mmol, 2 equiv). Yield: 30 mg, 90.6%;

*Complex **4d***: ^{1}H NMR (500 MHz, D$_2$O): δ=9.37 and 9.32 (d and d, J=6.4 and 6.45 Hz, 4H and 4H, H_a and H_e), 9.00 (d, J=8.0 Hz, 12H, $H_{q+q'}$), 8.33 (s, 4H, H_r), 8.25 (d, J=6.5 Hz, 4H, H_b/H_f), 8.19–8.15 (m, 8H, H_b/H_f and $H_{p1}+H_{p2}$), 7.98–7.92 (m, 12H, $H_{o1}+H_{o2}+H_{o'1}+H_{o'2}$), 7.49 (s, 4H, H_d), 5.56 ppm (s, 4H, H_c); MS (CSI): *m/z* calcd for [**4d**′-2(BF$_4$)]$^{2+}$: 625.5664; found: 625.5715.

*Complex **5d***: ^{1}H NMR (500 MHz, D$_2$O): δ=9.70 and 9.44 (d and d, J=6.25 and 6.41 Hz, 8H and 8H, $H_{a'}$ and $H_{e'}$), 9.00 (d, J=8.0 Hz, 12H, $H_{q'}+H_q$), 8.44 (d, J=6.4 Hz, 8H, $H_{b'}$/H_f), 8.32 (s, 8H, $H_{r'}$), 8.09–8.03 (m, 16H, $H_{b'}$/$H_f+H_{p'1}+H_{p'2}$), 7.98–7.92 (m, 12H, $H_{o'1}+H_{o'2}+H_{o1}+H_{o2}$), 5.40 (s, 8H, $H_{d'}$), 4.73 ppm (s, 8H, $H_{c'}$); MS (CSI): *m/z* calcd for [**5d**′-3BF$_4$]$^{3+}$: 863.0903; found: 863.1007.

The mixture of **4d**′ and **5d**′ was prepared in a similar manner by using Pd(phen)(BF$_4$)$_2$ instead of Pd(phen)(NO$_3$)$_2$.

Acknowledgements

D.K.C. thanks the Department of Science and Technology, Government of India (Project No. SB/S1/IC-05/2014) for financial support. We are grateful to Mr. V. Ramkumar for collecting single-crystal X-ray diffraction data. S.P. and B.S.R. thank CSIR and UGC, India for research fellowships. S.K. thanks IIT Madras for a postdoctoral fellowship. J.S.M., J.L., and G.S.H. thank the Canadian Foundation for Innovation (CFI), the Natural Sciences and Engineering Research Council (NSERC) of Canada and the Fonds de Recherche de Québec en nature et en Technologie (FRQNT) for financial support. D.K.C. also thanks the Shastri Indo-Canadian Institute for financial support covering his visit to Montreal.

Keywords: catenane · dynamic equilibrium · molecular karabiners · palladium · self-assembly

[1] a) E. A. Neal, S. M. Goldup, *Chem. Commun.* **2014**, *50*, 5128 – 5142; b) J.-C. Chambron, J.-P. Sauvage, *New J. Chem.* **2013**, *37*, 49 – 57; c) J. F. Stoddart, *Chem. Soc. Rev.* **2009**, *38*, 1521 – 1529; d) J. F. Stoddart, *Chem. Soc. Rev.* **2009**, *38*, 1802 – 1820; e) G. A. Breault, C. A. Hunter, P. C. Mayers, *Tetrahedron* **1999**, *55*, 5265 – 5293.

[2] a) B. Champin, P. Mobian, J.-P. Sauvage, *Chem. Soc. Rev.* **2007**, *36*, 358 – 366; b) C. Dietrich-Buchecker, M. C. Jimenez-Molero, V. Sartor, J.-P. Sauvage, *Pure Appl. Chem.* **2003**, *75*, 1383 – 1393.

[3] a) M. J. Langton, P. D. Beer, *Acc. Chem. Res.* **2014**, *47*, 1935 – 1949; b) A. Caballero, F. Zapata, P. D. Beer, *Coord. Chem. Rev.* **2013**, *257*, 2434 – 2455.

[4] a) G. Gil-Ramírez, D. A. Leigh, A. J. Stephens, *Angew. Chem. Int. Ed.* **2015**, *54*, 6110 – 6150; *Angew. Chem.* **2015**, *127*, 6208 – 6249; b) N. H. Evans, P. D. Beer, *Chem. Soc. Rev.* **2014**, *43*, 4658 – 4683; c) M. Fujita, *Acc. Chem. Res.* **1999**, *32*, 53 – 61; d) C. O. Dietrich-Buchecker, J.-P. Sauvage, *Chem. Rev.* **1987**, *87*, 795 – 810.

[5] a) M. Xue, Y. Yang, X. Chi, X. Yan, F. Huang, *Chem. Rev.* **2015**, *115*, 7398 – 7501; b) C. J. Bruns, J. F. Stoddart, *Acc. Chem. Res.* **2014**, *47*, 2186 – 2199; c) F. Durola, V. Heitz, F. Reviriego, C. Roche, J.-P. Sauvage, A. Sour, Y. Trolez, *Acc. Chem. Res.* **2014**, *47*, 633 – 645.

[6] a) J. F. Ayme, J. E. Beves, C. J. Campbell, D. A. Leigh, *Chem. Soc. Rev.* **2013**, *42*, 1700 – 1712; b) R. S. Forgan, J.-P. Sauvege, J. F. Stoddart, *Chem. Rev.* **2011**, *111*, 5434 – 5464; c) G. F. Swiegers, T. J. Malefetse, *Chem. Rev.* **2000**, *100*, 3483 – 3537.

[7] a) F. L. Thorp-Greenwood, A. N. Kulak, M. J. Hardie, *Nat. Chem.* **2015**, *7*, 526 – 531; b) S.-L. Huang, Y.-J. Lin, Z. H. Li, G.-X. Jin, *Angew. Chem. Int. Ed.* **2014**, *53*, 11218 – 11222; *Angew. Chem.* **2014**, *126*, 11400 – 11404; c) S.-L. Huang, Y.-J. Lin, T. S. A. Hor, G.-X. Jin, *J. Am. Chem. Soc.* **2013**, *135*, 8125 – 8128; d) K. S. Chichak, A. J. Peters, S. J. Cantrill, J. F. Stoddart, *J. Org. Chem.* **2005**, *70*, 7956 – 7962; e) K. S. Chichak, S. J. Cantrill, A. R. Pease, S.-H. Chiu, G. W. V. Cave, J. L. Atwood, J. F. Stoddart, *Science* **2004**, *304*, 1308 – 1312.

[8] a) N. Ponnuswamy, F. B. L. Cougnon, G. D. Pantoş, J. K. M. Sanders, *J. Am. Chem. Soc.* **2014**, *136*, 8243 – 8251; b) C. Schouwey, J. J. Holstein, R. Scopelliti, K. O. Zhurov, K. O. Nagornov, Y. O. Tsybin, O. S. Smart, G. Bricogne, K. Severin, *Angew. Chem. Int. Ed.* **2014**, *53*, 11261 – 11265; *Angew. Chem.* **2014**, *126*, 11443 – 11447; c) J. E. Beves, C. J. Campbell, D. A. Leigh, R. G. Pritchard, *Angew. Chem. Int. Ed.* **2013**, *52*, 6464 – 6467; *Angew. Chem.* **2013**, *125*, 6592 – 6595; d) C. D. Pentecost, K. S. Chichak, A. J. Peters, G. W. V. Cave, S. J. Cantrill, J. F. Stoddart, *Angew. Chem. Int. Ed.* **2007**, *46*, 218 – 222; *Angew. Chem.* **2007**, *119*, 222 – 226; e) C. Peinador, V. Blanco, J. M. Quintela, *J. Am. Chem. Soc.* **2009**, *131*, 920 – 921.

[9] a) M. Fujita, N. Fujita, K. Ogura, K. Yamaguchi, *Nature* **1999**, *400*, 52 – 55; b) D. Samanta, P. S. Mukherjee, *J. Am. Chem. Soc.* **2014**, *136*, 17006 – 17009; c) T. Hasell, X. F. Wu, J. T. A. Jones, J. Bacsa, A. Steiner, T. Mitra, A. Trewin, D. J. Adams, A. I. Cooper, *Nat. Chem.* **2010**, *2*, 750 – 755; d) A. Westcott, J. Fisher, L. P. Harding, P. Rizkallah, M. J. Hardie, *J. Am. Chem. Soc.* **2008**, *130*, 2950 – 2951; e) M. Fukuda, R. Sekiya, R. Kuroda, *Angew. Chem. Int. Ed.* **2008**, *47*, 706 – 710; *Angew. Chem.* **2008**, *120*, 718 – 722; f) S. Freye, J. Hey, A. T. Galán, D. Stalke, R. H. Irmer, M. John, G. H. Clever, *Angew. Chem. Int. Ed.* **2012**, *51*, 2191 – 2194; *Angew. Chem.* **2012**, *124*, 2233 – 2237; g) M. Frank, J. Hey, I. Balciogou, Y.-S. Chen, D. Stalke, T. Suenobu, S. Fukuzumi, H. Frauendorf, G. H. Clever, *Angew. Chem. Int. Ed.* **2013**, *52*, 10102 – 10106; *Angew. Chem.* **2013**, *125*, 10288 – 10293; h) S. Freye, R. Michel, D. Stalke, M. Pawliczek, H. Frauendorf, G. H. Clever, *J. Am. Chem. Soc.* **2013**, *135*, 8476 – 8479.

[10] E. Wasserman, *J. Am. Chem. Soc.* **1960**, *82*, 4433 – 4434.

[11] a) A. Coskun, J. M. Spruell, G. Barin, W. R. Dichtel, A. H. Flood, Y. Y. Botrosghi, J. F. Stoddart, *Chem. Soc. Rev.* **2012**, *41*, 4827 – 4859; b) E. R. Kay, D. A. Leigh, F. Zerbetto, *Angew. Chem. Int. Ed.* **2007**, *46*, 72 – 191; *Angew. Chem.* **2007**, *119*, 72 – 196.

[12] a) D. A. Leigh, R. G. Pritchard, A. J. Stephens, *Nat. Chem.* **2014**, *6*, 978 – 982; b) J. E. Beves, D. A. Leigh, *Nat. Chem.* **2010**, *2*, 708 – 710; c) K. R. West, R. F. Ludlow, T. P. Corbett, P. Besenius, F. M. Mansfeld, P. A. G. Cormack, D. C. Sherrington, J. M. Goodman, M. C. A. Stuart, S. Otto, *J. Am. Chem. Soc.* **2008**, *130*, 10834 – 10835; d) C. D. Meyer, C. S. Joiner, J. F. Stoddart, *Chem. Soc. Rev.* **2007**, *36*, 1705 – 1723; e) R. S. Forgan, J. J. Gassensmith, D. B. Cordes, M. M. Boyle, K. J. Hartlieb, D. C. Friedman, A. M. Z. Slawin, J. F. Stoddart, *J. Am. Chem. Soc.* **2012**, *134*, 17007 – 17010; f) F. B. L. Cougnon, H. Y. Au-Yeung, G. D. Pantoş, J. K. M. Sanders, *J. Am. Chem. Soc.* **2011**, *133*, 3198 – 3207; g) C.-F. Chang, C.-J. Chuang, C.-C. Lai, Y.-H. Liu, S.-M. Peng, S.-H. Chiu, *Angew. Chem. Int. Ed.* **2012**, *51*, 10094 – 10098; *Angew. Chem.* **2012**, *124*, 10241 – 10245; h) Z. Niu, C. Slebodnick, H. W. Gibson, *Org. Lett.* **2011**, *13*, 4616 – 4619; i) M. Liu, S. Li, M. Hu, F. Wang, F. Huang, *Org. Lett.* **2010**, *12*, 760 – 763; j) S. Li, M. Liu, B. Zheng, K. Zhu, F. Wang, N. Li, X.-L. Zhao, F. Huang, *Org. Lett.* **2009**, *11*, 3350 – 3353; k) E. N. Guidry, S. J. Cantrill, J. F. Stoddart, R. H. Grubbs, *Org. Lett.* **2005**, *7*, 2129 – 2132; l) C. Lincheneau, B. Jean-Denis, T. Gunnlaugsson, *Chem. Commun.* **2014**, *50*, 2857 – 2860; m) S. Tung, C. Lai, Y. Liu, S. Peng, S. Chiu, *Angew. Chem. Int. Ed.* **2013**, *52*, 13269 – 13272; *Angew. Chem.* **2013**, *125*, 13511 – 13514; n) J. Ayme, J. Lux, J.-P. Sauvage, A. Sour, *Chem. Eur. J.* **2012**, *18*, 5565 – 5573; o) J. E. Beves, B. A. Blight, C. J. Campbell, D. A. Leigh, R. T. McBurney, *Angew. Chem. Int. Ed.* **2011**, *50*, 9260 – 9327; *Angew. Chem.* **2011**, *123*, 9428 – 9499; p) J. D. Crowley, S. M. Goldup, A.-L. Lee, D. A. Leigh, R. T. McBurney, *Chem. Soc. Rev.* **2009**, *38*, 1530 – 1541; q) K. M. Mullen, P. D. Beer, *Chem. Soc. Rev.* **2009**, *38*, 1701 – 1713; r) M. D. Lankshear, P. D. Beer, *Acc. Chem. Res.* **2007**, *40*, 657 – 668; s) P. D. Beer, M. R. Sambrook, D. Curiel, *Chem. Commun.* **2006**, 2105 – 2117; t) J. C. Barnes, A. C. Fahrenbach, D. Cao, S. M. Dyar, M. Frasconi, M. A. Giesener, D. Benítez, E. Tkatchouk, O. Chernyashevskyy, W. H. Shin, H. Li, S. Sampath, C. L. Stern, A. A. Sarjeant, K. J. Hartlieb, Z. C. Liu, R. Carmieli, Y. Y. Botros, J. W. Choi, A. M. Z. Slawin, J. B. Ketterson, M. R. Wasielewski, W. A. Goddard, J. F. Stoddart, *Science* **2013**, *339*, 429 – 433; u) D. Qu, H. Tian, *Chem. Sci.* **2011**, *2*, 1011 – 1015; v) H. Li, A. C. Fahrenbach, S. K. Dey, S. Basu, A. Trabolsi, Z. Zhu, Y. Y. Botros, J. F. Stoddart, *Angew. Chem. Int. Ed.* **2010**, *49*, 8260 – 8265; *Angew. Chem.* **2010**, *122*, 8436 – 8441.

[13] a) T. Rama, E. M. López-Vidal, M. D. García, C. Peinador, J. M. Quintela, *Chem. Eur. J.* **2015**, *21*, 9482 – 9487; b) C. Alvariño, A. Terenzi, V. Blanco, M. D. García, C. Peinador, J. M. Quintela, *Dalton Trans.* **2012**, *41*, 11992 – 11998; c) G. Koshkakaryan, K. Primal, J. He, X, Zhang, Z. Abliz, A. H. Flood, Y. Liu, *Chem. Eur. J.* **2008**, *14*, 10211 – 10218; d) Y. Liu, A. Bruneau, J. He, Z. Abliz, *Org. Lett.* **2008**, *10*, 765 – 768; e) J. Lu, D. R. Turner, L. P. Harding, L. T. Byrne, M. V. Baker, S. R. Battern, *J. Am. Chem. Soc.* **2009**, *131*, 10372 – 10373.

[14] a) C. S. Wood, T. K. Ronson, A. M. Belenguer, J. J. Holstein, J. R. Nitschke, *Nat. Chem.* **2015**, *7*, 354 – 358; b) H. Lee, P. Elumalai, N. Singh, H. Kim, S. U. Lee, K. W. Chi, *J. Am. Chem. Soc.* **2015**, *137*, 4674 – 4677; c) B. X. Colasson, J. P. Sauvage, *Inorg. Chem.* **2004**, *43*, 1895 – 1901; d) S. Lee, J. Huang, T. R. Cook, J. B. Pollock, H. Kim, K. H. Chi, P. J. Stang, *J. Am. Chem. Soc.* **2013**, *135*, 2084 – 2087; e) K. Yamashita, M. Kawano, M. Fujita, *J. Am. Chem. Soc.* **2007**, *129*, 1850 – 1851; f) V. Blanco, M. D. García, C. Peinador, J. M. Quintela, *Chem. Sci.* **2011**, *2*, 2407 – 2416; g) V. Blanco, M. Chas, D. Abella, C. Peinador, J. M. Quintela, *J. Am. Chem. Soc.* **2007**, *129*, 13978 – 13986; h) K. Yamashita, A. Hori, M. Fujita, *Tetrahedron* **2007**, *63*, 8435 – 8439; i) M. Chas, E. Pia, R. Toba, C. Peinador, J. M. Quintela, *Inorg. Chem.* **2006**, *45*, 6117 – 6119; j) J. Sagué, K. M. Fromm, *Cryst. Growth Des.* **2006**, *6*, 1566 – 1568; k) W. W. H. Wong, J. Cookson, E. A. N. Evans, E. J. C. McInnes, J. Wolowska, J. P. Maher, P. Bishop, P. D. Beer, *Chem. Commun.* **2005**, 2214 – 2216; l) M. Beyler, V. Heitz, J. P. Sauvage, *J. Am. Chem. Soc.* **2010**, *132*, 4409 – 4417.

[15] M. Fujita, F. Ibukuro, H. Hagihara, K. Ogura, *Nature* **1994**, *367*, 720 – 723.

[16] a) L. Chen, Q. Chen, M. Wu, F. Jiang, M. Hong, *Acc. Chem. Res.* **2015**, *48*, 201 – 210; b) M. Han, D. M. Engelhard, G. H. Clever, *Chem. Soc. Rev.* **2014**, *43*, 1848 – 1860; c) M. M. J. Smulders, I. A. Riddell, C. Browne, J. R. Nitschke, *Chem. Soc. Rev.* **2013**, *42*, 1728 – 1754; d) T. R. Cook, Y.-R. Zheng, P. J. Stang, *Chem. Rev.* **2013**, *113*, 734 – 777; e) N. B. Debata, D. Tripathy, D. K. Chand, *Coord. Chem. Rev.* **2012**, *256*, 1831 – 1945; f) R. Chakrabarty, P. S. Mukherjee, P. J. Stang, *Chem. Rev.* **2011**, *111*, 6810 – 6918.

[17] a) M. C. Naranthatta, D. Das, D. Tripathy, H. S. Sahoo, V. Ramkumar, D. K. Chand, *Cryst. Growth Des.* **2012**, *12*, 6012 – 6022; b) D. Tripathy, V. Ramkumar, D. K. Chand, *Cryst. Growth Des.* **2013**, *13*, 3763 – 3772; c) H. Dasary, R. Jagan, D. K. Chand, *Chem. Eur. J.* **2015**, *21*, 1499 – 1507; d) M. C. Naranthatta, V. Ramkumar, D. K. Chand, *J. Chem. Sci.* **2014**, *126*, 1493 – 1499; e) M. C. Naranthatta, V. Ramkumar, D. K. Chand, *J. Chem. Sci.* **2015**, *127*, 273 – 280.

[18] a) D. K. Chand, R. Manivanan, H. S. Sahoo, K. Jeyakumar, *Eur. J. Inorg. Chem.* **2005**, 3346 – 3352; b) H. S. Sahoo, D. K. Chand, N. B. Debata, *Inorg. Chim. Acta* **2007**, *360*, 31 – 38; c) S. Bandi, N. B. Debata, V. Ramkumar, D. K. Chand, *Inorg. Chem. Commun.* **2014**, *39*, 75 – 78.

[19] a) N. B. Debata, D. Tripathy, V. Ramkumar, D. K. Chand, *Tetrahedron Lett.* **2010**, *51*, 4449 – 4451; b) N. B. Debata, V. Ramkumar, D. K. Chand, *Inorg. Chim. Acta* **2011**, *372*, 71 – 78.

[20] M. Fujita, M. Aoyagi, F. Ibukuro, K. Ogura, K. Yamaguchi, *J. Am. Chem. Soc.* **1998**, *120*, 611 – 612.

[21] a) M. Fujita, J. Yazaki, K. Ogura, *J. Am. Chem. Soc.* **1990**, *112*, 5645 – 5648; b) K. Uehara, K. Kasai, N. Mizuno, *Inorg. Chem.* **2007**, *46*, 2563 – 2570; c) M. Fujita, O. Sasaki, T. Mitsuhashi, T. Fujita, J. Yazaki, K. Yamaguchi, K. Ogura, *Chem. Commun.* **1996**, 1535 – 1536; d) D. K. Chand et al., unpublished results.

[22] a) M. Fujita, Y. J. Kwon, S. Washizu, K. Ogura, *J. Am. Chem. Soc.* **1994**, *116*, 1151 – 1152; b) M. Aoyagi, K. Biradha, M. Fujita, *Bull. Chem. Soc. Jpn.* **2000**, *73*, 1369 – 1373; c) O. M. Yaghi, H. Li, T. L. Groy, *Inorg. Chem.* **1997**, *36*, 4292 – 4293.

[23] a) X.-B. Shao, X.-K. Jiang, X. Zhao, C.-X. Zhao, Y. Chen, Z.-T. Li, *J. Org. Chem.* **2004**, *69*, 899 – 907; b) P. Chellan, K. M. Land, A. Shokar, A. Au, S. H. An, D. Taylor, P. J. Smith, T. Riedel, P. J. Dyson, K. Chibale, G. S. Smith, *Dalton Trans.* **2014**, *43*, 513 – 526.

[24] a) K. Yamaguchi, *J. Mass Spectrom.* **2003**, *38*, 473 – 490; b) K. Yamaguchi, *Mass Spectrom.*, **2013**, *2*, S0012; c) J. He, Z. Abliz, R. Zhang, Y. Liang, K. Ding, *Anal. Chem.* **2006**, *78*, 4737 – 4740.

[25] Gaussian 09, Revision A.02, M. J. Frisch, G. W. Trucks, H. B. Schlegel, G. E. Scuseria, M. A. Robb, J. R. Cheeseman, G. Scalmani, V. Barone, B. Mennucci, G. A. Petersson, H. Nakatsuji, M. Caricato, X. Li, H. P. Hratchian, A. F. Izmaylov, J. Bloino, G. Zheng, J. L. Sonnenberg, M. Hada, M. Ehara, K. Toyota, R. Fukuda, J. Hasegawa, M. Ishida, T. Nakajima, Y. Honda, O. Kitao, H. Nakai, T. Vreven, J. A. Montgomery, Jr., J. E. Peralta, F. Ogliaro, M. Bearpark, J. J. Heyd, E. Brothers, K. N. Kudin, V. N. Staroverov, R. Kobayashi, J. Normand, K. Raghavachari, A. Rendell, J. C. Burant, S. S. Iyengar, J. Tomasi, M. Cossi, N. Rega, J. M. Millam, M. Klene, J. E. Knox, J. B. Cross, V. Bakken, C. Adamo, J. Jaramillo, R. Gomperts, R. E. Stratmann, O. Yazyev, A. J. Austin, R. Cammi, C. Pomelli, J. W. Ochterski, R. L. Martin, K. Morokuma, V. G. Zakrzewski, G. A. Voth, P. Salvador, J. J. Dannenberg, S. Dapprich, A. D. Daniels, O. Farkas, J. B. Foresman, J. V. Ortiz, J. Cioslowski, D. J. Fox, Gaussian, Inc., Wallingford CT, **2009**.

[26] H. S. Sahoo, D. K. Chand, S. Mahalakshmi, Md. H. Mir, R. Raghunathan, *Tetrahedron Lett.* **2007**, *48*, 761 – 765.

[27] J. Lu, D. R. Turner, L. P. Harding, S. R. Batten, *Inorg. Chem.* **2009**, *48*, 7525 – 7527.

[28] a) L. Allouche, A. Marquis, J.-M. Lehn, *Chem. Eur. J.* **2006**, *12*, 7520 – 7525; b) K. F. Morris, P. Stilbs, S. Johnson Jr, *Anal. Chem.* **1994**, *66*, 211 – 215.

[29] M. M. Candana, S. Eroğlu, S. Özbeya, E. Kendi, Z. Kantarci, *Spectrosc. Lett.* **1999**, *32*, 35 – 45.

[30] a) S. Wimmer, P. Castan, F. L. Wimmer, N. P. Johnson, *J. Chem. Soc. Dalton Trans.* **1989**, 403 – 412; b) H. D. K. Drew, F. W. Pinkard, G. H. Preston, W. Wardlaw, *J. Chem. Soc.* **1932**, 1895 – 1909.

[31] E. O. Stejskal, J. E. Tanner, *J. Chem. Phys.* **1965**, *42*, 288 – 292.

[32] D. Wu, A. Chen, C. S. Johnson Jr., *J. Magn. Reson. A* **1995**, *115*, 123 – 126.

[33] C. S. Johnson Jr., *Prog. NMR Spectrosc.* **1999**, *34*, 203 – 256.

[34] SAINT, version 7.06 a.; Bruker AXS Inc., Madison, Wisconsin, USA, **2008**.

[35] G. M. Sheldrick, SADABS, University of Göttingen, Germany, **2004**.

[36] G. M. Sheldrick, *Acta Crystallogr. Sect. A* **2015**, *71*, 3 – 8.

[37] L. J. Farrugia, *J. Appl. Crystallogr.* **2012**, *45*, 849 – 854.

[38] C. F. Macrae, P. R. Edgington, P. McCabe, E. Pidcock, G. P. Shields, R. Taylor, M. Towler, J. van de Streek, *J. Appl. Crystallogr.* **2006**, *39*, 453 – 457.

[39] A. L. Spek, *Acta Crystallogr. Sect. A* **2009**, *65*, 148 – 155.

Received: June 20, 2015
Published online on September 23, 2015